Differences in skeletal muscle NFAT activity in response to strength- and endurance training

Ragnhild Bugge

Thesis submitted for the degree of
Master of Science in Molecular Biosciences

60 credits

Department of Bioscience
Faculty of Mathematics and Natural Sciences

UNIVERSITY OF OSLO

June / 2017

Differences in skeletal muscle NFAT activity in response to strength- and endurance training

Ragnhild Bugge

Thesis submitted for the degree of
Master of Science in Molecular Biosciences

60 credits

Department of Bioscience
Faculty of Mathematics and Natural Sciences

UNIVERSITY OF OSLO

June / 2017

2017

Differences in skeletal muscle NFAT activity in response to strength- and endurance training

Ragnhild Bugge

http://www.duo.uio.no/

Print: Reprosentralen, University of Oslo

Acknowledgements

This master thesis was carried out at the Section of Cell Biology and Physiology at the University of Oslo under supervision of Professor Dr. Kristian Gundersen, Dr. Einar Eftestøl and Ivan Myhre Winje.

First, I would to thank Professor Kristian Gundersen for providing me with the opportunity to work in his laboratory. Further, I would like to thank my main supervisor Einar for his guidance and encouragement. I am very grateful for all your valuable feedback during the final phase of my master thesis. Ivan, thank you for your optimism and discussions.

I would also like to thank the rest of the Gundersen group, other members of the physiology department and my coworkers at the animal facility for creating a great social atmosphere.

I would like to thank my family, my mother Nanna and my late father Malvin, for all your unconditional love and teaching me the value of hard work and persistence. Thanks to my siblings, Magnus and Marit, for all your cheerfulness and big-sibling wisdom.

To all my friends, thank you for your support and great company.

Oslo, June 2017
Ragnhild Bugge

Abstract

Skeletal muscles are highly adaptive to changes in functional demand and initiates several biochemical and physiological adaptations to optimize muscle functionality according to the nature of exercise. Nuclear factor of activated T cells (NFAT) is a family of transcription factors that has been proposed to be important in both fiber type switching and load-mediated hypertrophy in skeletal muscle. However, the role of NFAT in skeletal muscle is still controversial.

NFAT proteins are demonstrated to be differentially activated by electrical stimulation. It has therefore been problematic to study NFAT activity in response to mechanical load *per se,* as the neural input to the muscles increases correspondingly with increased load *in vivo*. Hence, it is problematic to attribute changes in NFAT activity are solely to load. In response to endurance training, previous study proposes that NFAT is upregulated through assessing Cn activity. However, since NFAT is not the only downstream target of Cn, further investigations are needed to assess NFAT transcriptional activity during endurance training. The present study uses a *in vivo* strength training setup that separates mechanical load and electrical stimuli by applying different loading regimes on identically electrically stimulated muscles in sedated mice. The purpose of the present study was to investigate NFAT activity in response to strength training with different loading regimes relative to endurance training. NFAT activity was assessed in muscle tissue homogenates through luciferase activity in transgenic mice where expression of luciferase is controlled by the transcriptional activity of NFAT.

In the present study, basal luciferase levels confirmed that NFAT activity was higher in slow muscles. NFAT was shown to be differentially activated during different forms of exercise. Elevated luciferase activity in response to endurance training showed that NFAT activity was higher in both *gastrocnemius* and *soleus* after running. In response to strength training, NFAT activity was only found significantly upregulated after low load strength training in the slow *soleus* muscle. However, all of the other trained-groups showed a small non-significant increase in NFAT activity relative to untrained contralateral control muscles. The findings from the present study suggest that NFAT activity is mainly activated during endurance training such as running, and less during strength training. Further, increased mechanical loading during strength training seems to have no effect on NFAT activity.

Abbreviations

ApoCaM	Apocalmodulin
ATP	Adenosine triphosphate
BSA	Bovine serum albumin
Ca^{2+}	Calcium
CaM	Calmodulin
CCLB	Cell culture lysis buffer
CMV	Cytomegalovirus
Cn	Calcineurin
CsA	Cyclosporin A
DBD	DNA-binding domain
DMEM	Dulbecco's Modified Eagle Medium
E.Coli	*Escherichia coli*
EDL	*Extensor digitorum longus*
EDTA	Ethylenediaminetetraacetic acid
EGFP	Enhanced green fluorescent protein
GSK3β	Glycogen synthase kinase 3β
HEK-293	human embryonic kidney 293 cells
LB	Lysogeny broth
MEF2	Myocyte enhancer factor-2
mRNA	Messenger ribonucleic acid
mTOR	Mammalian target of rapamycin
MyHC	Myosin heavy chain
NES	Nuclear export signal

NFAT	Nuclear factor of activated T cells
NHR	NFAT-homology region
NLS	Nuclear localization signal
NO	Nitric oxide
NOS	Nitric oxide synthase
PBS	Phosphate-buffered saline
PI3K/Akt	Phosphatidylinositol 3-kinase/Protein Kinase B
PVDF	Polyvinylidene difluoride
RCAN1-4	Regulator of Calcineurin 1 Isoform 4
RLU	Relative light units
SR	Sarcoplasmic reticulum
TA	*Tibialis Anterior*
TAD	Transcriptional activation domains
TBS	Tris-buffered saline
TBS-T	Tris-buffered saline-Tween
X-Gal	5-bromo-4-chloro-3-indolyl-β-D-galactopyranoside

Table of Contents

List of Figures

1 Introduction

1.1 Skeletal muscle

Skeletal muscle is a post-mitotic tissue made through fusion of numerous myoblasts forming long multinuclear cells called muscle fibers (Figure 1). Skeletal muscles constitute 40 % of the total human body mass (Janssen et al., 2000) and consists of connective, vascular, and nerve axons. Controlled by the somatic nerve system, skeletal muscles are responsible for all voluntary movements through the sliding filament principle (Huxley, 1957). Muscle fibers are excitable contractible cells specialized to convert chemical energy to mechanical energy when sarcomeres contract. Upon stimulation of a motor neuron, action potentials result in activation of muscle fibers and generation of tension through cross-bridge cycling between myosin and actin in the presence of Ca^{2+} and hydrolysis of ATP (Figure 1).

Skeletal muscles are a mosaic of distinct fiber phenotypes with different amount of molecular myofibrillar proteins and of metabolic enzymes, and consequently, in their contractile properties (Pette & Staron, 1990). The fiber types are divided into slow- and fast-twitch, expressing MyHC1 and MyHC2 (2a, 2x and rodent specific 2b), respectively (Figure 1) (Schiaffino & Reggiani, 1994, 2011; Spangenburg & Booth, 2003).

A group of individual muscle fibers that are exclusively activated by a single motor neuron is together called a motor unit. Activated neurons innervating slow-twitch and fast-twitch fibers exhibit action potentials at relative low- and high frequencies, respectively (Hennig & Lomo, 1985). By increasing the firing frequency of action potentials, more force can be generated by individual muscle fibers. According to Henneman's size principle, the smooth and steady increase in muscle tension is attributed to recruitment of motor units by the order of size, which befalls from smallest to largest (Henneman et al., 1965). Increased recruitment is consequently from an increased neural input from motor units that leads to an initial activation of slow-twitch fatigue resistant fibers, followed by fast twitch fatigue resistant fibers and finally activation of fast twitch highly fatigable muscle fibers (Conwit et al., 1999). Upon activation, the muscle may change its length (isotonic) or remain the same (isometric) (Figure 1). An isometric contraction maintains the same length since rise of tension doesn't reach the threshold

necessary to overcome the resistance. Conversely, during an isotonic contraction the muscle lengthen (eccentric) or shortens (concentric) while under a constant tension.

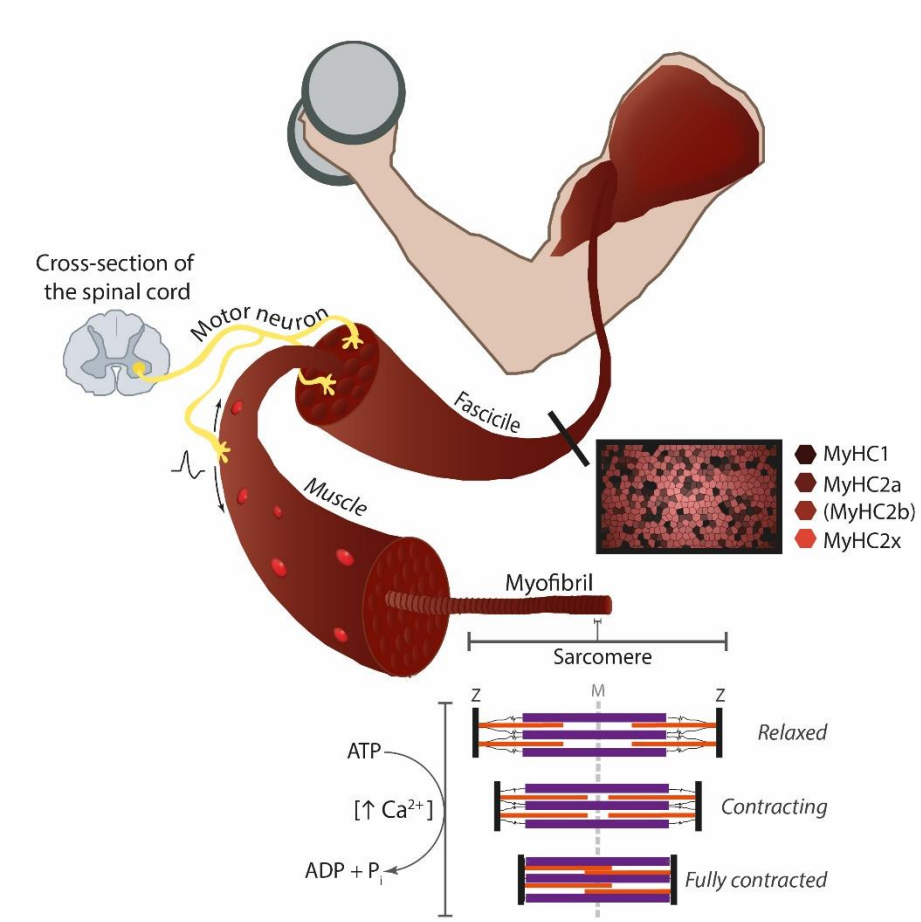

Figure 1: Schematic presentation of components in skeletal muscle

A skeletal muscle comprises of numerous fascicles that are further made up of muscle fibers. Muscle fibers are the elongated muscle cells, and are one of the few syncytia in vertebrates. Moreover, muscle fibers are divided into phenotypes commonly known as fast- and slow-twitch, with the latter appearing dark red due to higher amounts of myoglobin. Skeletal muscles are connected to several other tissues, e.g. motor neurons. A group of individual muscle fibers that are exclusively activated by a single motor neuron is called a motor unit. Upon activation of neurons, action potentials increase the intracellular concentration of Ca^{2+} which leads the sarcomeres to contract. Contraction occur when the myosin (purple) and actin (orange) filaments slide over each other by repeated cross-bridge cycles. In presence of Ca^{2+}, the myosin-binding site on actin is exposed and allows myosin to pull the actin filament towards M-line by ATP hydrolysis. Figure adapted in part from Silverthorn and Johnson (2016).

Sensitive to stimuli from various sources, adult skeletal muscle fibers hold the ability to adapt its phenotype in accordance with changes in stimuli and demand, called muscle plasticity (Gundersen, 2011). Skeletal muscle adapts to diverse stimuli through different downstream cascades, refining muscle properties by altering gene expression. However, the signaling transduction pathways linking external stimuli such as mechanical load to hypertrophic gene transcription is still largely elusive.

1.2 Hypertrophy

Muscle size is determent by protein turnover, with a catabolic- and anabolic net state resulting in muscle atrophy or hypertrophy, respectively (Millward et al., 1975; Rennie et al., 2004). Muscle atrophy is a decrease in muscle mass which occurs in a variety of pathological contexts, muscle wasting in the course of aging, and in lack of physical activity in healthy individuals (Goldspink, 1977; Paddon-Jones et al., 2006). Conversely, hypertrophy is the increase in individual myofibers size and strength, rather than an increase of fiber-number (hyperplasia) in response to hypertrophic stimulus (Goldberg, 1968).

In the late 90s, 70-kDa S6 protein kinase ($p70^{S6k}$) was the first molecular regulator of load-induced skeletal muscle hypertrophy to be identified (Baar & Esser, 1999). $p70^{S6k}$ is a downstream effector, and a member of the mammalian target of rapamycin (mTOR) pathway regulating muscle growth. The mTOR pathway is considered as the node in which muscles compute signals leading to a hypertrophic response. Several studies have shown that mTOR is essential for load-mediated hypertrophy (Bodine et al., 2001; DrummondFry et al., 2009; Goodman et al., 2011). mTOR is found in two protein complexes that differs in cellular localization and downstream targets, mTORC1 and mTORC2, regulating insulin-glucose uptake and muscle growth, respectively (Loewith et al., 2002). mTORC1 is activated by the GTPase Rheb by proposed pathways involving amino acids, hormones and mechanical stimuli (Coleman et al., 1995; DrummondDreyer et al., 2009; Hornberger, 2011; Kim & Guan, 2009). Aforementioned stimuli leads mTORC1 to promote hypertrophy by ribosome biogenesis and increased protein synthesis. Activated mTORC1 increase translational rate through phosphorylation of regulatory proteins $p70^{S6k}$ and 4E-BP1, which results in translational initiation by ribosomes (Holz et al., 2005). Moreover, mTORC1 signaling is suggested to regulate the elongation step of translation via $p70^{S6k}$ (X. Wang et al., 2001).

1.3 Exercise

In response to physical exercise, skeletal muscle adapts to the increased demand (Coffey & Hawley, 2007; Gundersen, 2011). The alteration of muscle mass in response to strength training was already studied in the late 60s (Goldberg, 1968, 1969). Muscles are highly responsive to changes in functional demands, and several biochemical and physiological adaptions are initiated to optimize muscle functionality. These adaptions may include e.g. fiber phenotype transitions, hypertrophy, vascularization, and increased mitochondrial density. Moreover, skeletal muscle shows a differentiated response to distinct exercise such as resistance and endurance training (Nader & Esser, 2001).

1.3.1 Endurance training

Endurance training is characterized by prolonged low-frequency activity, associated with both physiological and biochemical adaptions within the muscle tissue (Dudley et al., 1982). Endurance training has been reported to induce a fiber type switch from fast to slow phenotype (Allen et al., 2001). This mode of exercise also induces angiogenesis, with increased capillary density surrounding the working muscle (Andersen & Henriksson, 1977; Ingjer, 1979). In addition, the ability to utilize oxygen and produce ATP is enhanced as result of exercise induced mitochondria biogenesis and myoglobin synthesis (H. Wu et al., 2002). Myoglobin transports oxygen from capillaries to mitochondria, thus facilitating aerobic respiration. Endurance training is generally not associated with hypertrophy while resistance training commonly results in hypertrophy (Kraemer et al., 1995).

1.3.2 Resistance training

Resistance training is characterized by high-frequency activity, and is a potent stimulator of muscle protein synthesis and consequently muscle growth (McCall et al., 1996). Strength training is also accompanied with a fiber type switch towards slow phenotype independent of increased mechanical load in sedated rats undergoing different strength training regimes receiving identical electrical stimulation (Eftestol et al., 2016). The assumption that greater resistance in form of heavier weights leads to larger muscles compared to light weights is generally accepted. However, it is problematic to attribute the increased hypertrophic response solely to load as the neural input co-varies with alterations in mechanical load.

In vivo models to study the effect of mechanical factors

Different *in vivo* models commonly used to study the effect of load in rodents e.g. synergist ablation and hind-limb suspension may be problematic as these are most likely accompanied with alterations in neural input from motor neurons. Therefore, it has been challenging to study the effect of mechanical load *per se* since it is difficult to separate these two closely connected stimuli. However, a progressive strength training apparatus called myograph enables the electrical and mechanical factors to be studied separately in sedated rodents (Caiozzo et al., 1992; Eftestol et al., 2016; Wong & Booth, 1988). In short, the myograph facilitate independent control of mechanical loading and electrical stimulation and can be used to investigate pathways in mechanotransduction when identical stimulation patterns are applied (More details given in section 3.3.6).

1.4 Mechanotransduction

Mechanotransduction enables muscles to sense external forces by converting mechanical stimuli into downstream biochemical signaling cascades (N. Wang et al., 2009). Remote from the initial trigger, downstream signaling cascades leads to an altered gene expression associated with e.g. hypertrophy (Yamada et al., 2012).

Initial mechanosensing units in skeletal muscle are largely an elusive chapter in muscle physiology, however emerging evidence suggests involvement of several structural proteins associated and within the contractive apparatus, in addition to stretch-activated ion channels (SACs) in the sarcolemma (Burkholder, 2007; Gumerson & Michele, 2011; Vandebrouck et al., 2007). Force transmission is suggested to occur both in a longitudinal and lateral direction in skeletal muscles (P. A. Huijing, 1999; Peter A. Huijing, 2003). Lateral force transmission is demonstrated to be transferred through large membrane-cytoskeletal complexes called costameres. Costameres comprises of a multi-subunit complex called Dystrophin-Glycoprotein-Complex (DGC) which links the contracting apparatus via desmin to the sarcolemma and extracellular matrix (ECM) (Figure 2). Studies suggest that most of lateral force transmission is transferred through this pathway via DGC (Ramaswamy et al., 2011; Street, 1983).

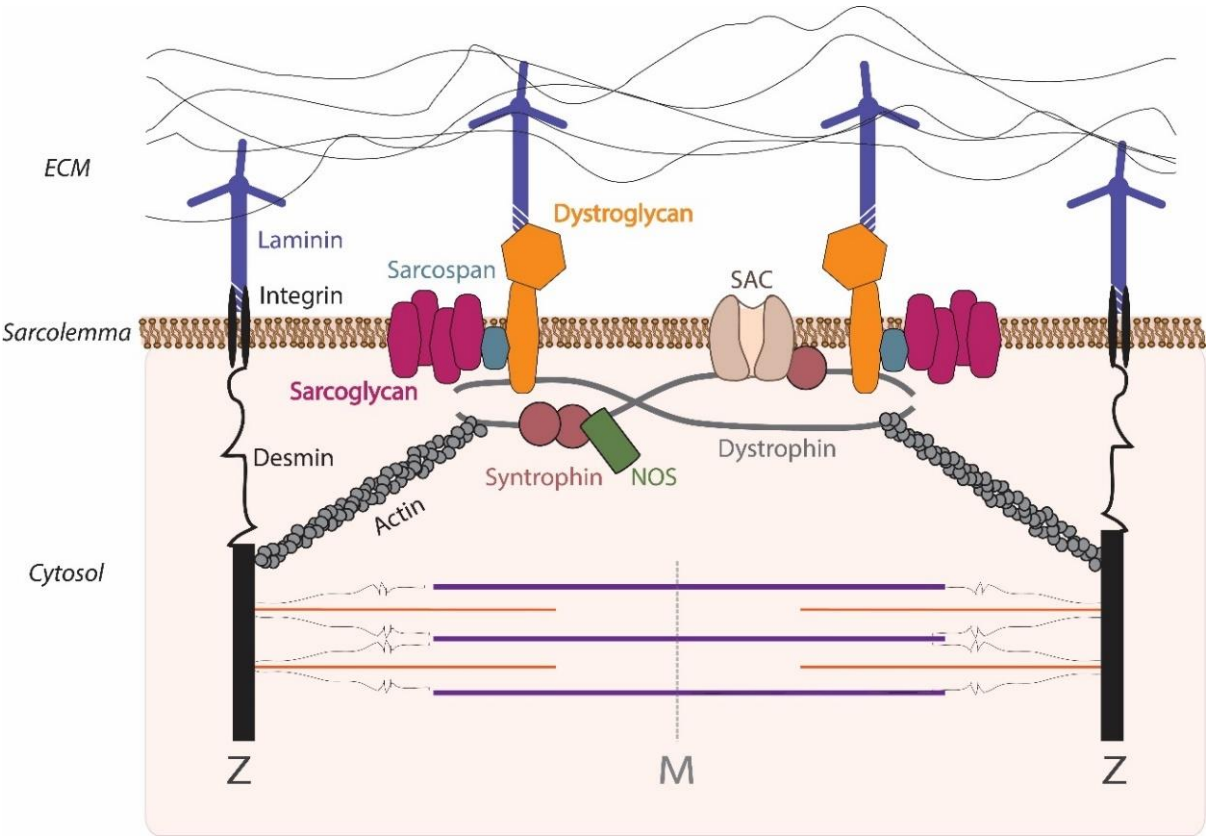

Figure 2: Schematic presentation of different proteins associated with the DGC
DGC is a multi-subunit protein complex spanning from the sarcomeres to the ECM and is important in transferring lateral forces in muscle. One type of SACs is shown to be physically associated with DGC and is activated in response to lateral forces. Once activated, Ca^{2+} initiates numerous of signaling cascades e.g. Cn-NFAT pathway. Figure adapted from Hughes et al. (2015); (Vandebrouck et al., 2007).

Mechanical stress is also thought to trigger influx of Ca^{2+} by direct sarcolemmal damage or via SACs (Clarke et al., 1993; Yeung et al., 2005). One type of SACs is demonstrated to be physically associated with DGC through the subunits dystrophin and α-1syntrophin (Figure 2) (Vandebrouck et al., 2007). Ca^{2+} influx is crucial in excitation-contraction coupling, but Ca^{2+}signaling is also important in excitation-transcription coupling. Clearly, there are a myriad of calcium effectors, however the Ca^{2+}-dependent phosphatase Cn and its downstream effectors has been proposed to be activated through SACs (Zobel et al., 2007). Cn activity have been demonstrated to play an important role in e.g. fiber phenotype transitions, hypertrophy and muscle development. One downstream effector of Cn, a family of transcription factors called Nuclear factor of activated T cells (NFAT), are suggested to be linked to both fiber type switching and hypertrophy (Chin et al., 1998; Delling et al., 2000; Semsarian et al., 1999). The muscle-specific subcellular localization of NFAT in unstimulated fibers has been reported to be at the Z-disks of the sarcomere. A

colocalization study of NFATc1-GFP and α-actinin showed an aligned and repetitive pattern perpendicular to the length of the fiber (Y. Liu et al., 2001). NFAT has earlier been reported to dock on Cn in unstimulated cells, and consistent findings show that Cn is localized at the Z-disk via calsarcin binding during resting conditions in muscle fibers (Frey et al., 2000; Garcia-Cozar et al., 1998).

However, there are little direct evidence that NFAT is part of mechano-induced hypertrophy in skeletal muscle. Nevertheless, mechanotransduction has been more extensively studied in cardiac muscle where the Cn/NFAT-pathway is shown to participate in pathological hypertrophy (Finsen et al., 2011; Wilkins et al., 2004). Recent findings of Eftestol et al. (2016) demonstrated *in vivo* that increased mechanical loading enhanced the hypertrophic response in muscles of rats receiving identical electrical stimulation patterns. Moreover, Cn/NFAT activity was assessed through protein levels of Regulator of Calcineurin 1 Isoform 4 (RCAN1-4) which was observed to be 2.6-fold higher in the *Tibialis anterior* (TA) muscle only in response to high load strength training (Eftestol et al, unpublished results). NFAT is a potent regulator of RCAN1-4 due to a cluster of 15 NFAT binding sites in this isoform promoter region (J. Yang et al., 2000), thus RCAN1-4 can be used as a measure of NFAT activity. During paralysis, RCAN1-4 is one of the most strongly downregulated genes which is not reversed by electrical stimulation (Y. Wu et al., 2013). This, together with the recent unpublished finding by Eftestol et al. implicates participation of NFAT signaling in mechano-induced hypertrophy in skeletal muscle. However, further research is needed to elucidate NFAT involvement by assessing NFAT activity directly in response to mechanical stimuli.

1.5 NFAT

The NFAT proteins are a family of transcription factors evolutionary related to Rel/NF-κB (GraefGastier et al., 2001), and are exclusively found in the vertebrate genome for the first time about 500 million years ago (H. Wu et al., 2007). NFAT was initially described as central activators of T-lymphocyte in the late 80s (Shaw et al., 1988), but was later recognized as important mediators in several other processes in a wide range of tissues (Crabtree & Olson, 2002). The NFAT family consist of five members denoted NFATc1 through NFATc5. With exception of NFATc5, which is regulated by osmotic stress (Miyakawa et al., 1999), the NFAT family comprise of closely related proteins regulated through Ca^{2+}-signaling (Hoey et al., 1995). In the literature, the family members are known under several names and the different family members also exists in several isoforms with alternative 3' and 5' splicing variants (Table 1) (Vihma et al., 2008). The focus of this thesis is on NFATc1-4 and their possible involvement in mechano-induced hypertrophy in skeletal muscle.

Table 1: Nomenclature and regulation of the different NFAT family members.

Protein	Other names	NFAT isoforms	Regulation
NFATc1	NFAT2, NFATc	IA, IB, VIII, IXL, IXS	Ca^{2+}/calcineurin
NFATc2	NFAT1, NFATp	IA-IIS, IA-IIS-III, IB-IIL, IB-IIL-III, IB-IIS-III, VIIa	Ca^{2+}/calcineurin
NFATc3	NFAT4, NFATx	IB, ΔXa	Ca^{2+}/calcineurin
NFATc4	NFAT3	VI, VIi, IXi, IXL	Ca^{2+}/calcineurin
NFATc5	TonEBP		Osmotic stress

Table adapted from Hogan et al. (2003) and expression of different NFATc1-4 isoforms in mice are based on Vihma et al. (2008).

1.5.1 NFAT protein structure

The NFATc1-4 family members share central conserved domains, but they display great variation in their N- and C-terminal regions. The highly-conserved DNA binding domain (DBD), also known as the Rel-homology domain, allows the different proteins to bind to the same DNA sequence in promoter regions. However, since the DBD of NFAT proteins lacks a loop compared to the homologous Rel-domain, NFAT is shown to cooperate with transcriptional partners or forms homodimers for adequate DNA binding and transcription initiation (Bates et al., 2008; Jin et al., 2003). Distinct NFAT transcriptional partners is proposed to interact with specific domains of NFAT. The moderately conserved NFAT-

homology region (NHR), is highly phosphorylated and restricted to the cytoplasm under basal conditions, having four classes of serine-rich sequence motifs phosphorylated (Hogan et al., 2003). Moreover, NHR contains two Cn-docking sites, kinase-docking sites and nuclear translocation sequences. The nuclear translocation sequences are recognized by the nuclear transportation machinery which shuttles proteins through the nuclear pore complex. Flanking the conserved domains are two highly variable transcriptional activation domains (TADs) with great distinction amongst both different NFAT proteins and splice variants. The TADs are putative sites for interactions between distinct NFAT proteins and associated transcriptional partners. (Mognol et al., 2016). Thus, it is probable that the diverse functions of NFAT in various tissues could be attributed to highly variable TADs and cooperation with different transcriptional partners.

1.5.2 NFAT signaling pathway

Under basal conditions, phosphorylation sequester NFAT in the cytoplasm localized at the Z-disks where it remains inactive until an appropriate stimulus leads to transient elevated Ca^{2+} levels (Figure 3). Contracting muscle fibers generate spikes in cytoplasmic Ca^{2+} as a result of opening of several different ion channels in the plasma membrane and Ryanodine receptor 1 (RYR1) in sarcoplasmic reticulum (SR) membrane initiates the influx and release of Ca^{2+}, respectively (Figure 3, [1-2]). Sarco/endoplasmic reticulum Ca^{2+}-ATPase (SERCA) localized in the membrane of SR actively pumps Ca^{2+} back into SR lumen, leading the muscle to relax as the cytosolic Ca^{2+} levels drops (Gundersen et al., 1988).

Periods of sustained transient elevation of intracellular Ca^{2+} (e.g. during exercise) leads to activation of calmodulin (CaM) when it binds up to four Ca^{2+} -molecules (Figure 3, [3]) (Faas et al., 2011). CaM is a potent intermediate calcium-binding messenger protein which interacts with several proteins. Further, CaM has been shown to regulate Ca^{2+}-release from SR, depending on Ca^{2+}-impact, by sensitizing or inhibiting RYR1. ApoCaM (CaM without bound Ca^{2+}) sensitize RYR1 while calcified CaM inhibits further release from RYR1 (Moore et al., 1999; Rodney et al., 2000). Further, activated CaM binds to the regulatory domain of Cn, subsequently activating its phosphatase activity by a conformational change within the catalytic domain of Cn (Figure 3, [4]) (Yang & Klee, 2000; Ye et al., 2013). Cn is a serine/threonine phosphatase that dephosphorylates the serine-rich N-terminal region of NFAT, thus exposing the nuclear import signal (NLS)

(Crabtree et al., 2002; Loh et al., 1996). Cn is also shown to translocate to the nucleus in smooth muscle, thus maintaining the dephosphorylated state of NFAT proteins (Jabr et al., 2007). However, Cn- and subsequently NFAT activity can be inhibited by several proteins, e.g. RCAN1-4, and the commonly used immunosuppressant drug CsA (Dunn et al., 1999; Vega et al., 2002). With NLS exposed, NFAT proteins translocate through nuclear pores after recognition by the nuclear import machinery (Figure 3, [5]) (Belfield et al., 2006). However, dephosphorylation and nuclear localization may be insufficient for NFAT dependent transcription as the DNA-binding capacity of NFAT is poor. Adequate DNA binding with subsequent transcription is shown to be through formation of homodimers, or in cooperation with transcriptional partners like GATA2 and MEF2 (Figure 3, [6]) (Musaro et al., 1999; Hai Wu et al., 2001). When stimuli ceases, the drop in the intracellular Ca^{2+} level terminates NFAT signaling by rephosphorylation of the regulatory domain by nuclear kinases like casein kinase 1 or 2 and glycogen synthase kinase 3β (Okamura et al., 2004; Shen et al., 2007). Phosphorylation masks the NLS and leads the nuclear export signal (NES) to be recognized by nuclear export receptor CRM1, which mediates cytoplasmic translocation and hinders nuclear accumulation (Figure 3, [8]) (Kehlenbach et al., 1998).

The critical regulatory step in the NFAT pathway is presumed to be dephosphorylation of Cn, thus exposing the NLS followed by nuclear translocation facilitated by nuclear import machinery. However, opposing findings poses an alternative pathway where phosphorylated NFAT bypasses Cn and translocate to the nucleus (Figure 3, [9]) (Okamura et al., 2000; Shen et al., 2006; Terui et al., 2004). In cultured adult mouse skeletal muscle fibers, NFATc1 is shown to translocate to the nucleus under resting conditions without dephosphorylation of Cn (Shen et al., 2006). Other studies have also observed Cn-independent translocation of NFATc2 in HELA and BHK cells (Okamura et al., 2000; Terui et al., 2004). Supporting evidence *in vivo* show translocation of NFATc1 independently of Cn activation in skeletal muscle fibers (Shen et al., 2006). Since the nuclear pore complex are impermeable for proteins bigger than ~40kDa, large proteins are dependent on recognition by nuclear transport receptors to shuttle between cytosol and nucleus. This implying the existence of another dephosphorylation mechanism that facilitates unmasking of the NLS and enables nuclear shuttling. However, the details regarding the Cn-independent translocation are still unknown.

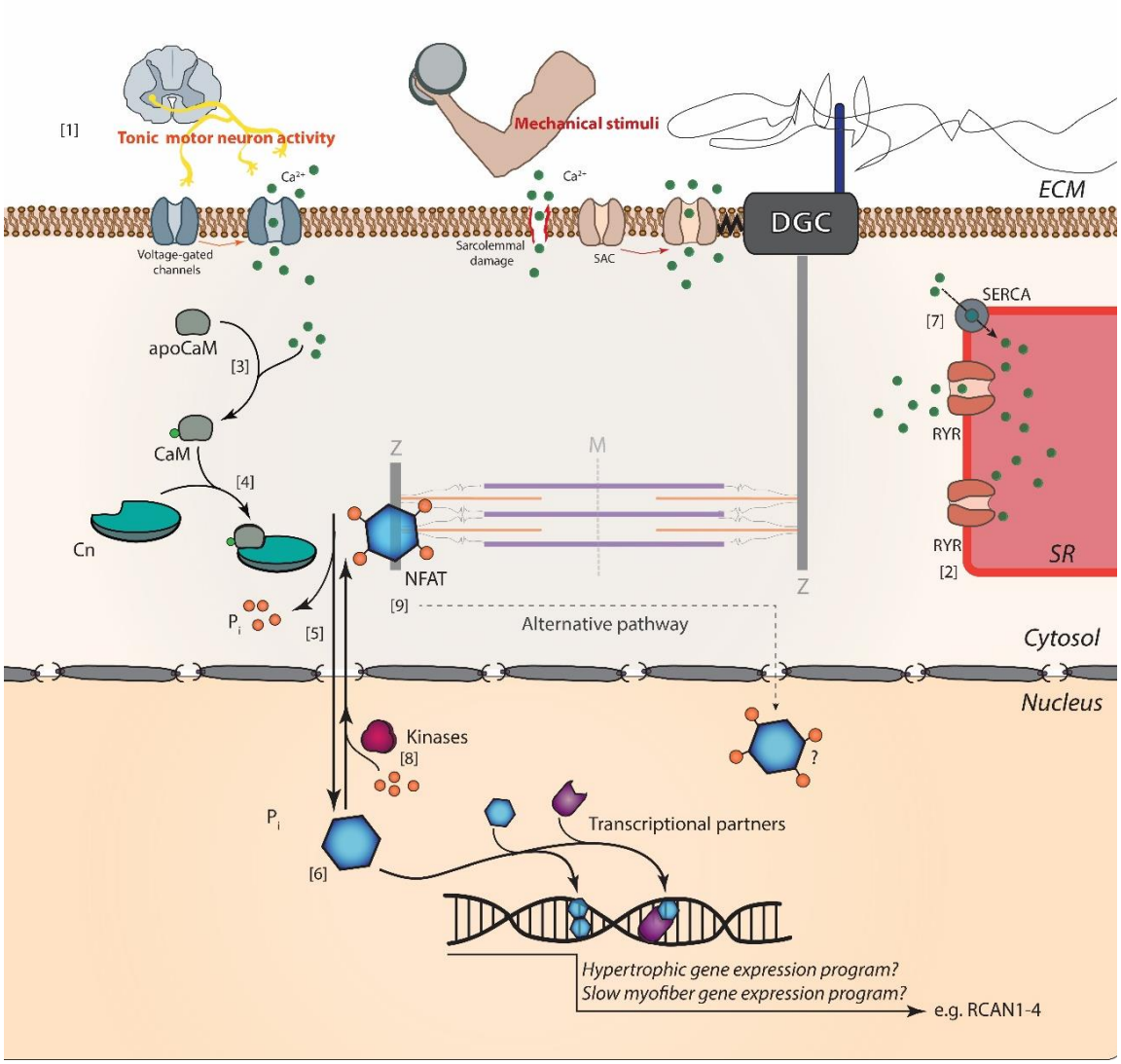

Figure 3: A schematic overview of proposed NFAT pathway

[1] Neural and mechanical stimuli triggers Ca^{2+}-channels in the sarcolemma to open voltage and stretch-activated channels, respectively. During resistance training, sarcolemmal damage may occur and contribute to increased intracellular concentration of Ca^{2+}. Lateral forces are proposed to be sensed through DGC. One type of SACs is reported to be a part of DGC (details shown in Figure 2). [2] Increased intracellular levels initiates Ca^{2+} release from SR. [3] ApoCaM binds Ca^{2+} ions, consequently activating CaM. Further, apoCaM can also sensitive RYR-governed Ca^{2+} release from SR. [4] CaM activates Cn by binding to the regulative subunit. Further, calcified CaM can also inhibit further Ca^{2+} release from SR. [5] Activated Cn dephosphorylated sequestered NFAT proteins, consequently unmasking the NLS which is recognized by the nuclear translocation machinery and translocate NFAT through nuclear pores. [6] NFAT forms homo- or heterodimers to initiate transcription for its target genes. [7] SERCA pumps Ca^{2+} ions through active transport into the SR lumen. [8] A drop of Ca^{2+} levels inactivate Cn, and NFAT is subsequently phosphorylated by nuclear kinases. NES is recognized by CRM1 which mediates nuclear export of NFAT, thus termination of NFAT dependent transcription. [9] Alternative pathway of NFAT which bypasses Cn dephosphorylation and leads to nuclear translocation (details are not known). Figure based on: (Benavides Damm & Egli, 2014; Rodney et al., 2000; Tidball, 2005; Vandebrouck et al., 2007)

1.5.3 The distribution and expression level of NFAT proteins in skeletal muscle

All NFAT family members regulated through Ca^{2+}-signaling have been shown to be present at the RNA and protein level in skeletal muscle (Calabria et al., 2009; Hoey et al., 1995; Stephanie A. Parsons et al., 2003; Vihma et al., 2008). Some studies report an overall higher expression levels of NFATc1 and NFATc3 proteins than the other NFAT family members, in adult skeletal muscle (Hoey et al., 1995; Swoap et al., 2000). Moreover, the relative expression of the different family members is shown to be variable in fast- and slow muscles. In particular, NFATc3 is found to be more abundant in the fast muscle *Extensor digitorum longus* (EDL) relative to the slow muscle *soleus*. Overall, slow myofibers is reported to have higher NFAT activity compared to fast fibers (McCullagh et al., 2004) and nuclear localization has also been reported to higher in *soleus* than in EDL (Swoap et al., 2000).

The nucleocytoplasmic distribution of NFAT proteins is an indicator of its activity state because, as previously mention, the transcription factor is translocated to the nucleus in response to dephosphorylation and consequently activation of Cn. Muscle-specific subcellular localization of NFAT in unstimulated fibers has been reported to be at the Z-lines of the sarcomeres. A colocalization study of NFATc1-GFP and α-actinin showed an aligned and repetitive pattern perpendicular to the length of the fiber (Y. Liu et al., 2001). NFAT has earlier been reported to dock on Cn in unstimulated cells, and consistent findings show that Cn is localized at the Z-line via the binding of calsarcin during resting condition in fibers (Frey et al., 2000; Garcia-Cozar et al., 1998).

Several studies have investigated NFAT transcriptional activity through nuclear translocation and this research have mainly been performed by stimulating cells with different electrical pattern. However, the experiments discussed below do not assess the mechanical factors that might co-vary in response to electrical stimuli with different frequency pattern. Therefore, it is important to keep in mind that NFAT activity in response to different electrical pattern could possibly be influenced by alterations in mechanical factors.

Different NFAT family members has been shown *in vivo* to be differentially sensitive to electrical stimulation with different nucleocytoplasmic distribution in adult muscle fibers (Calabria et al., 2009). For instance, in response to slow 20Hz-pattern NFATc1-4 was

found to be nuclear accumulated, while a fast 100Hz-pattern facilitated nuclear shuttling of NFATc3-4, although NFATc2 was only observed in a fraction of nuclei (Calabria et al., 2009). In cultured adult muscle fibers of mice, consistent results also only observe translocation of NFATc1 in response to electrical simulation that mimics slow fiber type neural input (Y. Liu et al. (2001). NFATc4 was shown to be predominantly located in the nucleus of skeletal muscles, both during resting and stimulating conditions, implying that the basal activity-level of Cn is efficient to dephosphorylate NFATc4, and/or a possible slow rephosphorylation rate by nuclear kinases (Calabria et al., 2009). The mechanisms of which different NFAT family members differentially translocate is still unknown.

The time course of nuclear localization of NFATc1 coupled to GFP in response to electrical stimulation have been investigated in cultured adult skeletal fibers (Y. Liu et al., 2001). Two different stimulation protocols were tested, continuous 10 Hz and 5-second trains of 10 Hz every 50-second, with the latter resulting in longer nuclear localization. This is in agreement with other studies reporting that NFAT is activated by transient levels of Ca^{2+} Upon 5 minutes of electrical stimuli, both protocols induce NFATc1 translocation with a steady increase of nuclear signal within the 30-minute protocol. The intranuclear fluorescence signal remained constant approx. 10-20 minute after cessation of stimulation, and had a half-life of 1.3-9 hours depending on stimulation protocol. Nuclear localization was still apparent at 2 hours after ended stimulus. Moreover, intranuclear distribution of NFAT proteins is suggested to be concentrated/organized in distinct foci. In cultured mouse adult muscle fibers, NFATc1 is reported to be accumulated in nuclear foci after nuclear translocation by electrical stimulation. Moreover, these accumulated sites of NFATc1 appears to evade nucleoli in nucleus (Y. Liu et al., 2001).

1.5.4 The role of NFAT proteins in skeletal muscle

During development of skeletal muscle tissue, the various stages of myogenesis from a quiescent satellite cell to a mature myotube requires several important transcription factors. Investigations of myogenesis *in vitro* show no measurable differences of distinct NFATc1-4 protein levels (Abbott et al., 1998). However, nuclear translocation in response to ionomycin treatment during different stages of myogenesis were distinct among different NFAT family members. Ionomycin increase Ca^{2+} influx and mobilization, subsequently activating the Cn/NFAT-pathway as previously described.

Thus, ionomycin treatment led only NFATc3 to nuclear translocate in myoblasts, while translocation of NFATc1-2 was observed only in myotubes. Further, NFATc2 translocation was further limited to newly formed myotubes (Abbott et al., 1998).

In vivo studies have implemented knockout mice models to elucidate the functions of different NFAT family members in skeletal muscle (de la Pompa et al., 1998; Horsley et al., 2001; Kegley et al., 2001). NFATc1 knockouts have severe defects in cardiogenesis resulting in embryonic lethality (de la Pompa et al., 1998). NFATc2 knockouts led to muscle atrophy compared to wild-type mice, correlated to a reduction of individual muscle fiber cross-section area in both fast (33%) and slow (44%) phenotype fibers in *soleus*. Investigations of possible fiber type alterations by immunohistochemistry revealed a significant decrease of fibers expressing MyHC1 by 5%, but not in fibers expressing MyHC2 (Horsley et al., 2001). Moreover, knockouts of NFATc3 also display muscle atrophy compared to wild-type mice. However, this is correlated to a decrease in muscle fiber number, not individual fiber CSA, and is not attributed to a specific fiber type. In contrast to NFATc2 knockouts, the fiber type allocation are not altered in NFATc3 knockouts (Kegley et al., 2001). NFATc4 target knockouts exhibit no special phenotype. However, observations under *in situ* hybridization of NFATc4 expression revealed a significant overlap with NFATc3, the closest homologous family member. Double knockout mice of NFATc3-4 resulted in embryonic lethality (GraefChen et al., 2001). Thus, indicating that these family members may have redundant functions as the effect is concealed when one is knocked out, while double knockout is lethal in mice.

The role of NFAT in adult skeletal muscle is controversial. Several studies have demonstrated the requirement of NFAT activity in correlation to fiber type transitions, but not hypertrophy, and *vice versa*. Several lines of evidence suggest that NFAT activity is required for fiber type transitions of muscle fiber *in vivo* (Chin et al., 1998; Naya et al., 2000; S. A. Parsons et al., 2004). The correlation between different NFAT proteins and transcription of fiber type specific gene programs in adult skeletal muscle has been investigated *in vivo* by RNAi-mediated gene silencing and MyHC reporter constructs (Calabria et al., 2009). As previously mentioned, each NFAT family member exists in several isoforms, thus to facilitate effective silencing, a specific siRNA for a mutual gene region for all splice variants is needed. Previously, it has been suggested that NFATc1 is the main regulator of slow MyHC1 expression (Ehlers et al., 2014), however this may be an oversimplification as Calabria et al. (2009) observed a strong inhibitory effect on

MyCH1 expression with all NFATc1-4 specific siRNA knockdowns. Suggesting that the different NFAT family members have nonredundant roles in regulating slow MyCH1 expression. Different fast MyHC2 (2a, 2x and 2b) isoforms in EDL were observed to be more independently influenced by different NFAT family members. First, MyHC2a expression was deeply affected by siRNA knockdowns of NFATc2-4, but not NFATc1. Moreover, analogous combination of NFAT proteins were central in MyHC2x expression, though NFATc3 knockdown had a higher inhibitory effect in MyHC2a than MyHC2x. Last, the fastest MyHC isoform 2b were only inhibited by NFATc4-specific siRNA, while silencing by NFATc1-3 siRNA were indistinguishable from control (Calabria et al., 2009). These findings elucidate a more complex framework of NFAT modulation of distinct MyHC isoform expression. However, several lines of evidence indicate NFATc1 to be a specific regulator of slow MyCH1 expression with translocation facilitated only by slow pattern specific electrical stimulation.

Cn/NFAT signaling have also been suggested to promote hypertrophy. As previously mentioned, increased proteins levels of endogenous NFAT activity reporter RCAN1-4 was only observed upregulated in response to high load strength training (Eftestol et al., unpublished). Moreover, the robust hypertrophy predicted with mechanical overloaded *plantaris* was abolished with subcutaneous administration of the specific calcineurin inhibitors CsA (25mg/kg) or FK506 (3-5mg/kg) in mice (Dunn et al., 1999). In contrast, another study excludes Cn/NFAT activity in the hypertrophic response to mechanical overloading in *plantaris* as Cn inhibitors (CsA (15mg/kg) and FK506 (3mg/kg)) did not block observed hypertrophy (Bodine et al., 2001). These findings might suggest that even a downregulated NFAT activity could be sufficient to promote hypertrophy. Further, other studies do not observe hypertrophy or atrophy in response to overexpression or knockout of Cn, respectively (Naya et al., 2000; Stephanie A. Parsons et al., 2003). Still, several emerging lines of evidence indicate that Cn/NFAT signaling supports hypertrophy in slow muscle fibers (Oh et al., 2005; Sakuma et al., 2008; Talmadge et al., 2004). *In vitro* study with C2C12 cells demonstrate IGF-1 mediated myotube growth suggested to be under regulation of Cn/NFAT signaling as CsA treatment blunt hypertrophy (Semsarian et al., 1999).

1.5.5 Target genes of NFAT proteins

Transcriptional regulation by NFAT has been linked to several genes such as myoglobin (Chin et al., 1998), troponin I (Chin et al., 1998), RCAN1-4 and MyHC isoforms. Further, transcription of several target proteins has been demonstrated to be in cooperation with different transcriptional partners, e.g. NFATc2-3 and MyoD is suggested to cooperate in myogenesis (Armand et al., 2008). Moreover, GATA2 was found to bind NFATc1 specifically, but not NFATc2, to induce myocyte hypertrophy *in vitro* (Musaro et al., 1999). This additional layer of modulation of NFAT dependent transcription by association by different transcriptional partners to distinct NFAT family members and isoforms further complicates the quest of illuminating NFAT signaling. Collectively, the intricate modulation in context with fundamental uncertainties in regards of the nature of activating stimuli originates from electrical activity or mechanical factors makes NFAT signaling in muscle ambiguous. Nevertheless, NFAT is suggested to be important in transcription of several crucial muscle specific genes and have a proposed role in both fiber type switching and hypertrophy. Therefore, by overcoming the fundamental uncertainties of the origin of transcriptional activating stimuli by implicating experimental setup allowing separation of close regulated would illuminate a more clearer picture of the role of NFAT

2 Aims of the Study

The role of NFAT in skeletal muscle is a matter of controversy. The close relationship between electrical and mechanical factors has hampered the quest to elucidate NFAT activity in response to specific stimuli. Emerging evidence of the molecular mechanisms of mechanotransduction propose NFAT as a downstream effector candidate. This thesis is based on previous findings performed in the Gundersen group (Eftestol et al., 2016), where a target gene of NFAT, RCAN1-4, was found upregulated in response to mechano-induced hypertrophy (Eftestol et al, unpublished results). Further, this study sought to investigate any changes in NFAT activity during endurance training. The aim of this study was to investigate possible differences in NFAT activity in response to endurance- and strength training with different loading regimes.

Hypotheses:

I. Activation of NFAT through translocation to nuclei differs between fast and slow muscles in response to varying load during strength training.
II. NFAT activity is higher in slow than in fast muscles.
III. NFAT activity increases with increased mechanical loading during strength training.
IV. Successive strength training sessions increases NFAT activity compared to one session.
V. Endurance training increases NFAT activity.

3 Material and Methods

3.1 NFATc1-4-EGFP expression vectors

The NFATc1-4-EGFP plasmids (GenScript) were a kind gift from Dr. Ida G. Lunde (Institute for Experimental Medical Research, Oslo University Hospital, Norway). The NFATc1-4 genes are cloned into the backbone expression vector pEGFP-N1 in frame with an EGFP gene (Clonetech) (Figure 4).

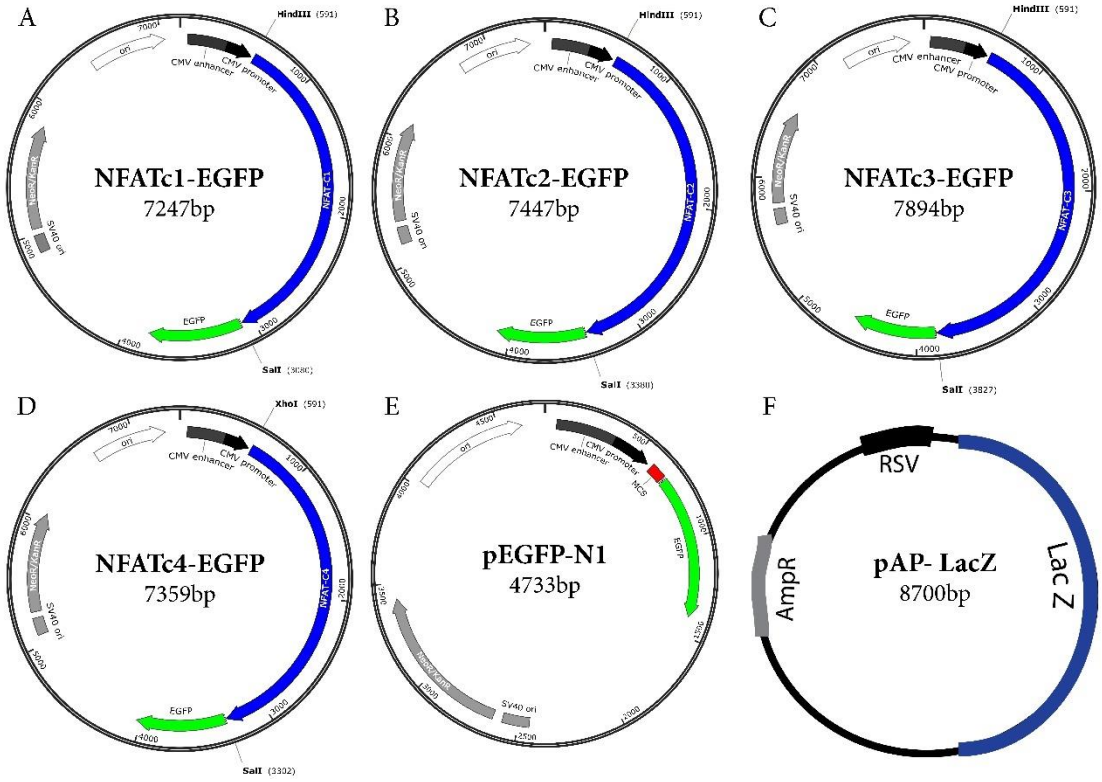

Figure 4: Expression vectors for study of in vivo localization of NFAT1-4
(A-D) NFATc1-4-EGFP, a gift from Dr. Ida G. Lunde. Experimental plasmids expressing the different NFAT family members fused to EGFP for visualization under control of a Cytomegalovirus (CMV) promoter for enhanced mammalian expression. (E) Backbone plasmid pEGFP-N1 (Clonetech) expressing EGFP through a CMV promoter. (F) Transfection control plasmid pAP-LacZ (gift from N. Gautam) with the Rous sarcoma virus promoter. (A-E) Plasmid maps were generated in SnapGene® software (from GSL Biotech; available at snapgene.com).

Amplification of NFATc1-4-EGFP plasmids was performed through transformation of competent TOP10 *E.coli* cells. The bacteria were grown overnight at 37°C on LB-agar plates with kanamycin as selection marker. Further, the cells were grown in LB media for 18hours before purification following supplier protocol Plasmid Megaprep System (Qiagen). The plasmids were verified by restriction digest analysis (data not shown) and sanger sequencing of the different NFAT genes (performed by GATC Biotech).

3.2 Cell culture

3.2.1 Culturing HEK-293 cells

The HEK-293 cell line was established by Graham et al. (1977) from human embryonic kidney cells in the late 70s. Cell culture was incubated at 37 °C in an atmosphere of 5 % CO_2 in Dulbecco's Modified Eagle Medium (Invitrogen) supplemented with 10 % fetal bovine serum and 1 % Penicillin-Streptomycin. Depending on cell confluence, the cells were split 1:4 every 4-5th day with trypsin-EDTA. When sub-culturing, old culture medium was discarded before successive washing with 1X Dulbecco's phosphate-buffered saline to ensure complete removal of old medium containing trypsin inhibitor. Trypsin-EDTA was added and incubated for 3 minutes at 37 °C and 5 % CO_2, before new medium was added to neutralize trypsin-EDTA and feed the cells. After cell counting, an appropriate number of cells were transferred to multi-well plates for transfection.

3.2.2 Verification of NFATc1-4-EGFP plasmids

Transfection of NFATc1-4-EGFP and pEGFP-N1 was carried out in six well plates (Costar) in accordance with the protocol of Lipofectamine™ 3000 kit (Invitrogen). Lipofectamine treated HEK293 cells was used as a negative control (data not shown), while pEGFP-N1 transfected cells served as a positive control. After 24 hours, further analysis was performed by fluorescent microscopy and western blotting as described below.

3.2.2.1 Fluorescence imaging of transfected cell culture

24 hours after transfection, the cells were checked for NFATc1-4-EGFP expression. Cells were placed on ice and fixed with 4 % PFA with successive Hoechst staining at room temperature and washed with PBS. Cells were imaged using a camera (Canon, EOS 60D) connected to an upright fluorescence microscope (BX50WI, Olympus). Pictures were taken in a dark room with 40x water immersion objective with XF11 and XF22 filter cubes to visualize DNA and EGFP, respectively. Photo processing was conducted in Photoshop CS6 (Adobe).

The expression of all fusion proteins except NFATc3-EGFP was verified by fluorescent microscopy (Figure 5A-D). The subcellular localization of fusion proteins seems to be mainly in the cytoplasm but are also found localized to nuclei in HEK293 cells.

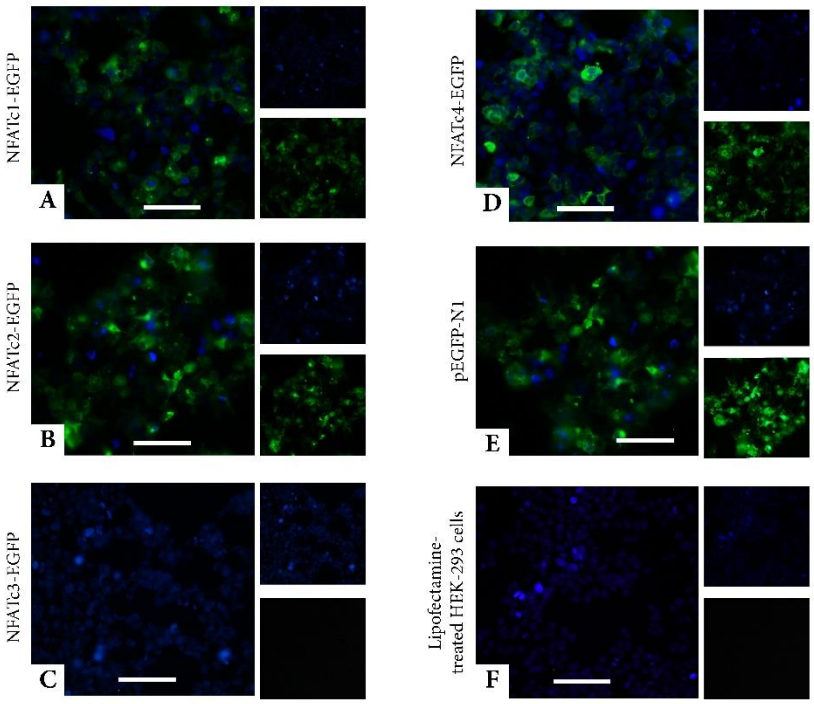

Figure 5: Intracellular expression of NFATc1-4-EGFP fusion proteins in HEK293 cells
HEK293 cells were observed under a fluorescence microscope 24 hours after transfection and examined for expression of NFATc1-4-EGFP. (A-D) HEK293 cells transfected with NFATc1-4-EGFP. (C) No expression of NFATc3-EGFP was observed. (E) HEK293 cells transfected with backbone plasmid pEGFP-N1 served as a positive control. (F) HEK293 lipofectamine 3000 treated cells served as a negative control. Nuclei stained with Hoechst, Picture taken at 40X. Scale bars: 100µM.

3.2.2.2 SDS-PAGE and Western Blotting

Transfected HEK293 cells were removed of old medium and subsequently washed twice while on ice with 1 ml cold PBS. SDS buffer were added to the cell plates (see appendix), scraped off by a plate-scraper (Costar) and transferred into 1.5 ml Eppendorf tubes, followed by 5 minutes of sonication at room temperature and centrifugation at 13000 G for 5 minutes at 4 °C. Sodium dodecyl sulfate polyacrylamide gel electrophoresis (SDS-PAGE) and western blotting were performed in accordance with the instruction manual (Bio-Rad). Supernatants and protein ladder (Kaleidoscope™ Standards, Bio-Rad) were loaded on a Mini-PROTEAN TGX gel (Bio-Rad) and run for 1 hour (PowerPac Universal, Bio-Rad). The gel was blotted onto a nitrocellulose membrane (Bio-Rad) for 10 minutes at 1.3A/25V (Trans-Blot Turbo, Bio-Rad). The blotted membrane was blocked in 5 % skimmed milk powder in TBS-T (see appendix) for 1 hour at room temperature. Blocking was followed by immunostaining with primary rabbit antibody against GFP diluted 1:2000 and Glyceraldehyde-3-phosphate dehydrogenase (GAPDH)

diluted 1:5000 for 1 hour. Then immunostaining with ECL Peroxidase labeled secondary antibody against rabbit (GE) diluted 1:2000 in TBS with 5 % skimmed milk at 4°C was performed. After immunostaining, the membrane was washed 3 times for 10 minutes each in TBS-T and lastly rinsed with TBS. The blot was visualized by addition of ECL Western Blotting Substrate Pierce™ (Thermo Fischer) using the Carestream Health Molecular Imaging System.

Expression of all NFAT-EGFP fusion proteins except NFATc3-EGFP was also confirmed by western blot (Figure 6). The SDS-PAGE mobility of the present NFAT-EFGP fusion proteins was as anticipated based on the information provided by the manufacture GenScript, with NFATc1-EGFP, NFATc2-EGFP and NFATc4-EGFP migrating at ~120, ~130 and ~130kDa, respectively. Cells transfected with pEGFP-N1 expression vector display two separate bands of EGFP migrating at ~30kDa, and might be due to post translational modifications alternating the SDS-PAGE mobility of EGFP.

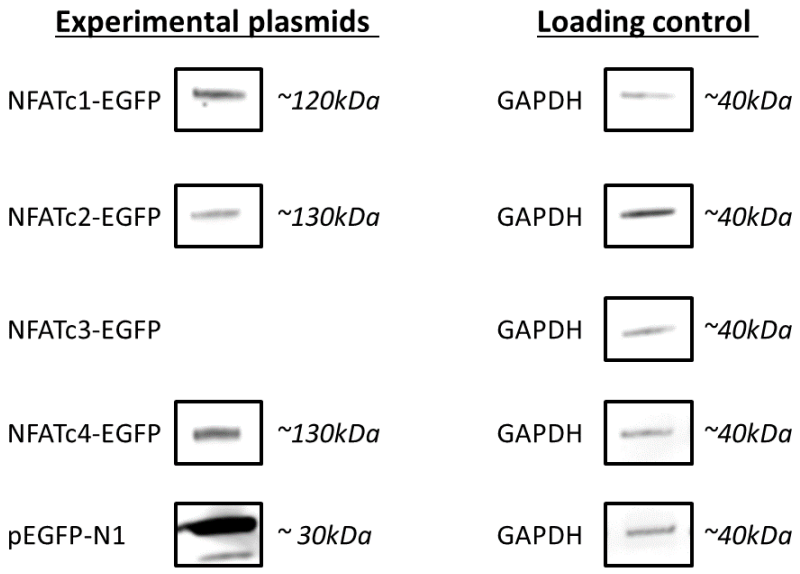

Figure 6: Western blot of NFATc1-4-EGFP fusion proteins in HEK293 cells.
Western blot of HEK293 cells transfected with distinct NFATc1-4-EGFP fusion plasmids and pN1-EGFP. Expression of fusion proteins and EGFP was visualized by immunostaining with anti-GFP antibody. In HEK293 cells transfected with NFATc3-EGFP, no band was observed for the fusion protein while the loading control showed the appropriate band size. The backbone plasmid pEGFP-N1 expressing EGFP served as a positive control and observed as two separate bands at ~30 kDa. HEK293 cells treated with transfection reagent lipofectamine 3000 was used as a negative control (data not shown). Staining with anti-GAPDH served as a loading control to confirm equal loading across the gel. n=1.

3.3 Animal experiments

3.3.1 Ethical considerations

Animal procedures were reviewed and approved by the Norwegian Animal Research Authority and were conducted in accordance with the Norwegian Animal Welfare Act of December 20th, 1974, no. 37, chapter VI, sections 20-22, and the Regulation of Animal Experimentation of January 15th, 1996. As required by the Norwegian Food Safety Authority, an animal researcher certificate (FELASA C) was obtained before proceeding with the animal experiments in this thesis.

3.3.2 Animals

All animals were held and cared for by the animal research facility at the Department of Biosciences during the experiments. Ventilated cabinets (Scanbur Technology) were used to house animals and reduce the exposure to e.g. microorganisms and other contaminations. The animals had standard living arrangement for rats and mice with up to 4 and 10 individuals living together, respectively. Polycarbonate cages for rats (35x55x19 cm) and mice (19x13x38 cm) were filled with woodchip bedding (Scanbur AS), and furthermore enriched with red polycarbonate houses or play tunnels. The living conditions were held standardized with regulated light cycles at 12h/12h intervals accompanied with stable temperature at 22±2 ºC and a humidity level at 55±10 %. Food in form of RM1 pellets (Special Diets Services) and water were given *ad libitum*.

Male Sprague Dawley rats weighing between 350-450 g were electroporated with different NFAT-EGFP fusion proteins. Fusion proteins were intended to differentiate the transcriptional activity of distinct NFAT proteins in response to different strength training regimes. This study was not completed as the transfection efficiency was poor and resulted in fiber degradation (discussed in section 5.1).

NFAT-luciferase reporter mice (FVB/J) (Wilkins et al., 2004), kindly provided by Dr. Jeffery D. Molkentin (Cincinnati Children`s Hospital Medical Center, Cincinnati, OH). The transgenic region consists of three regions; a cluster of nine consensus NFAT binding sites, a TATA-box from the α-MyHC gene and a firefly luciferase (*Photinus pyralis*) reporter gene from pGL-3Basic (Promega). Female mice 2 months of age weighing between 19-25 g were used in this thesis to assess NFAT spatiotemporal transcriptional activity in response to mechano-induced hypertrophy and voluntary endurance training.

3.3.3 Anesthesia

Preceding all animal procedures, animals were anesthetized by placing them inside an anesthesia-chamber with isoflurane gas at 3 % per 0.8 l/min (MSS Isoflurane with the SurgiVet Active Ecacuation System) until deep anesthesia was induced. Deep anesthesia was always confirmed by pinching the metatarsus region of the foot and witnessing the absence of the leg withdrawal reflex. Preceding surgical procedures, animals where transferred to an appropriate gas mask where anesthesia was maintained with inhalation of gas anesthesia containing isoflurane in air at 1.5-2 % per 0.6-0.8 l/min. Further, the respiratory rate of the sedated animal was observed and considered when regulating the administration of anesthetics during experiments. After the experiments, the animals were sacrificed under deep anesthesia by neck dislocation.

3.3.4 Surgical procedures and excision protocol

After deep anesthesia was confirmed, the leg hair was removed in two successive steps with an electrical shaver and application of hair removal cream (Veet). The animal was laid on its back with a given leg fixed onto a plastic bloc by pinning it into a locked position. The fixed leg was rinsed with 70 % ethanol before making an incision of 1-1.5cm at the medial side of the leg exposing, EDL and *soleus* for excision. Thereafter, the animal was turned to access and excise the *gastrocnemius* muscle on the backside of the leg. Last, the kidneys and heart was excised. The surgery area was continuously kept wet by applying Ringer-Acetate solution. All tissue samples were weighted and subsequently snap frozen in liquid nitrogen at -196 °C and stored at -80 °C until further analysis.

3.3.5 *In vivo* electroporation of EDL and *soleus*

Co-transfection of NFAT-EGFP and pAP-LacZ reporter plasmids was performed by *in vivo* electroporation of *soleus* and EDL in male Sprague Dawley rats. Electroporation of tissue enables electropermeabilization (Potter, 1988) and co-transfection is demonstrated to yield a concurrent high co-expression of proteins (Rana et al., 2004).

Animals were sedated as previously mentioned before surgically exposing EDL and *soleus*. An insulin syringe (0.3ml, BD Micro-Fine™, VWR) was used to inject 30 µl of 1 µg/µl DNA solution (see appendix) into the belly of the muscle. Two silver electrodes (1cmx1mm) were adjusted according to the muscle diameter, and placed perpendicular to fiber lengths on each side of the muscle. An electrical field was applied using a pulse

generator (Pulsar 6bp, Fredrick Haer & Co) and the electrical charge was registered by an analogue oscilloscope (Gould Advance). Electrical stimuli were delivered in 5 trains with 1 second intermission, and the electrodes were moved along the muscle during the intermission. Each train consisted of 1000 bipolar pulses with amplitude of 150 V/cm, 200 µs in each direction. Following electroporation, the wound was closed with sutures (Softsilk, S-1172, 12 mm, Syneture) and rinsed with 70 % ethanol before the animal was placed back into its cage to heal. At different timepoints after electroporation, the muscles were study *in vivo* by fluorescence microscope (section 3.8.2), excised and slightly stretched between two pins attached to a plastic bloc and subsequently stained for X-gal (section 3.7) and imaged (section 3.8.1).

3.3.6 *In vivo* strength training

In vivo strength training was performed essentially as previously described by Eftestol et al. (2016). The myograph setup (Figure 7) is a modified version of a Whole Animal Test System (Aurora Scientific Inc.), and was adjusted for experiments involving mice by optimization of the electrical stimulation protocol, and exchanging the knee-holders and foot pedal. The experiments were controlled and monitored through ASI600A software (Aurora Scientific). The muscles of interest were stimulated with an optimized stimulation protocol (Figure 8) using skin-electrodes connected to a pulse generator (Pulsar 6bp-a/s) with the stimulation timing controlled through the software. The foot pedal was connected to a computer-controlled DC motor, enabling the mechanical parameters to be monitored and excursion to be controlled.

Preceding all *in vivo* strength training experiments, mice were anesthetized with inhalation gas anesthesia containing isoflurane in air at 1.5 % per 0.4 l/min. Animals were removed of leg hair before locking the right leg in a knee-holder and foot pedal. Electrical stimulation was delivered non-invasive through two skin electrodes (2x2 mm) covered with electrode gel (Spectra 360; Parker Laboratories). The electrodes were positioned on the skin over the plantar-flexors muscle group (GAS and SOL) on each side of the right leg. The stimulation voltage was set at 30 V to ensure supramaximal activation. The contralateral leg was used as a normal intra-animal control to correct for possible effects of e.g. sedation and inter-animal differences. To prevent a decline in body temperature for the duration of the 62-minute long experiment, mice were placed on a homothermic blanket system. Animals that underwent one training session were placed back into their

cage before muscles were harvested at four hours later (explained in section 3.5). Mice that completed three training sessions had one rest day in between each session before muscles were harvested four hours after the last training session. Excised tissue was snap-frozen in liquid nitrogen, and stored at -80 °C as previously described.

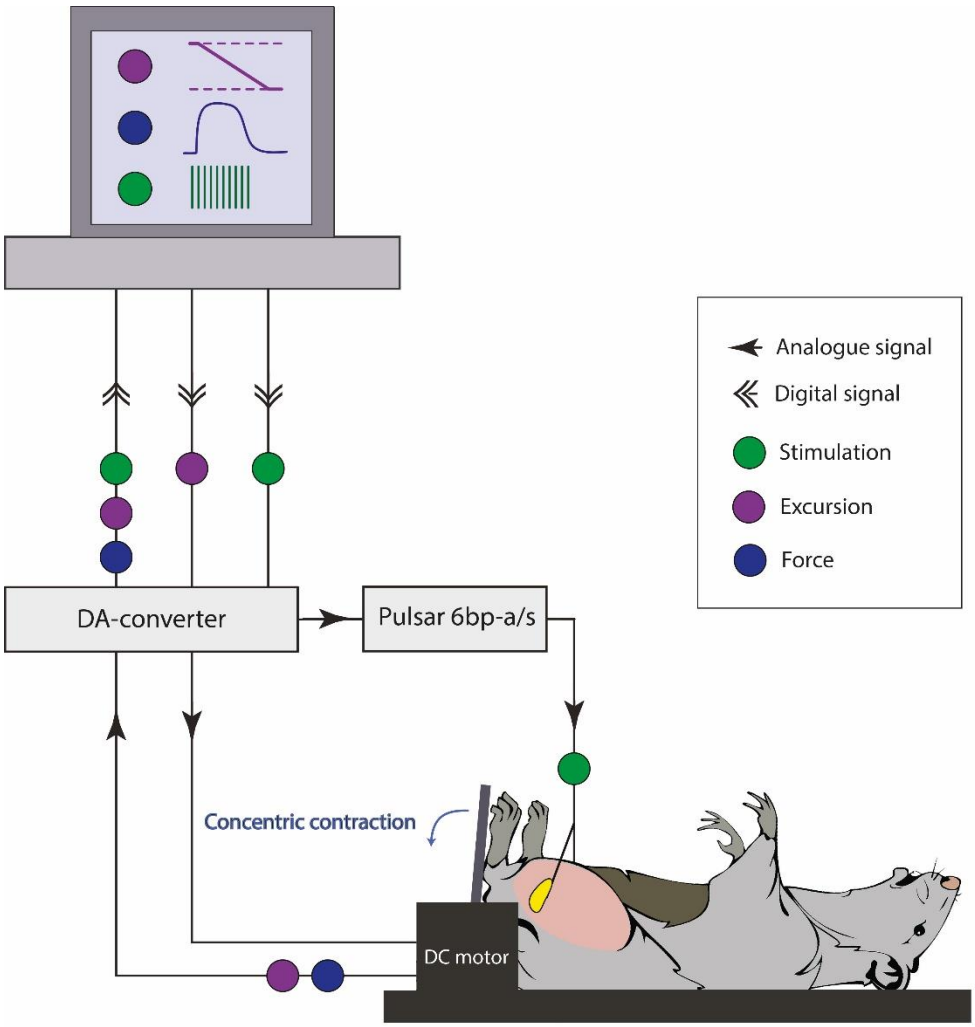

Figure 7: Schematic illustration of the myograph strength training setup

An example of a low load strength training setup for *gastrocnemius* and *soleus* (plantar-flexors muscle group). The training session was monitored on a PC with the Aurora Scientific ASI600A software. An optimized stimulation protocol (green) for mice was sent from the software to a pulse generator (Pulsar 6bp-a/s) before an analog stimulation pattern was delivered to the muscle through skin electrodes. Simultaneous, a digital signal with excursion instructions (purple) passes through the DA-converter which forwards an analog signal to the DC-motor. The foot pedal is connected to the DC-motor which senses the excursion and force (blue), thus the signals are sent back to the converter and subsequently, together with the stimulation protocol, to the software. This enables consecutively monitoring of the different parameters for the duration of the experiment. In the top right corner is a QR-code which gives access to a video-clip demonstrating both high and low load strength training.

Under identical electrical stimulation (Figure 8), animals were divided into two groups with different loading regimes. The high load group performed an isometric contraction, while the low load group performed a fast-concentric contraction producing 50-60 % peak force compared to high load. Even though different contractions have been shown to have different neural activities (Linnamo et al., 2003; Moritani et al., 1987), several studies demonstrate that load rather than contraction type is important for the hypertrophic response (Garma et al., 2007; Wong et al., 1988). The 62-minute stimulation protocol was divided into three 20-minute series with 1 minute intermission, each series contain six 150-second sets of contraction trains with 1 minute intermission. Each set was made up of a contractions train with 30 contractions, each separated with 5-second intermission. Each contraction lasted approx. 120 milliseconds, and was generated by 10 consecutive impulses at 150 Hz. As previously mentioned in the introduction, resistance training is characterized by high-frequency activity, and therefore the stimulation pattern consisted of impulses at 150 Hz to resemble the physiological electrical activity in muscles during strength training.

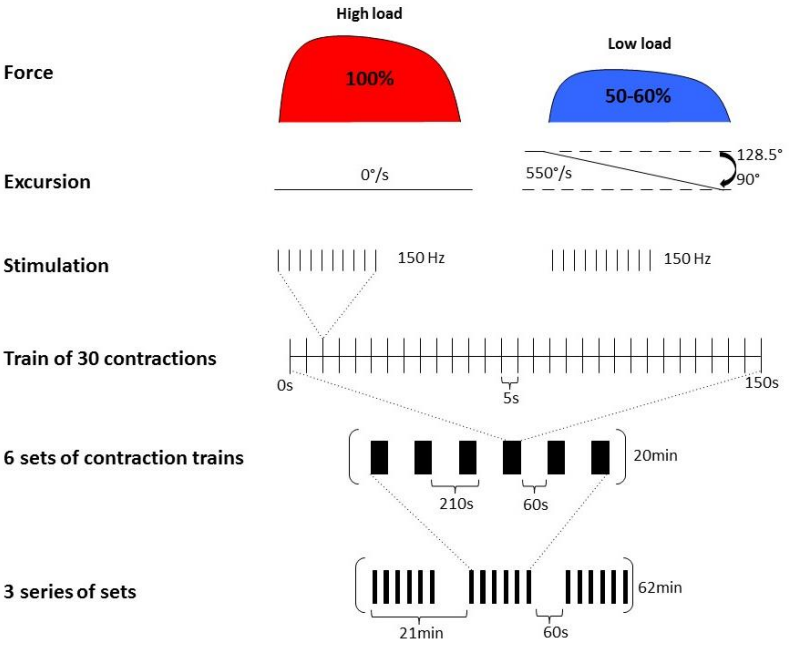

Figure 8: Schematic overview of the training regime.
An overview of the force, excursion and stimulation pattern during the training session for the different experimental groups. The predicted force was 100 % and 50-60 % during an isometric and fast-concentric contraction for the high and low load group, respectively. The stimulation pattern consisted of 10 consecutive impulses at 150 Hz yielding a tetanic contraction of approx. 120ms. One series of contractions consisted of 30 contractions with 5s intermissions lasted 150s. A set was made up of 6 series with 1min intermission between each series lasting a total of 20min, and during the entire training session of 62min the mice completed 3 set with 1min intermissions. Figure adapted from Eftestol et al. (2016).

3.3.7 Voluntary endurance training with running wheel

Mice were housed individually into cages installed with a running wheel (16 cm, Trixie) for a period of 3-4 days until the running distance exceeded 10 km/night. The mice were monitored with a near infra-red video camera (Foscam) and running distance was registered with a cycling computer (Asaklitt) that converted number of wheel-rounds into linear distance covered (Figure 9). Running distance was calculated by multiplying the circumference in mm of the running wheel with π, thereafter rotations were multiplied with 0.000502 km. After the activity criteria of 10 km/night were met, muscle tissue was excised and snap frozen the following morning as previously described and stored at -80 °C. Film footage obtained from a representative selection of mice the night before tissue was harvested were analyzed for running activity pattern (Supplementary figure 1).

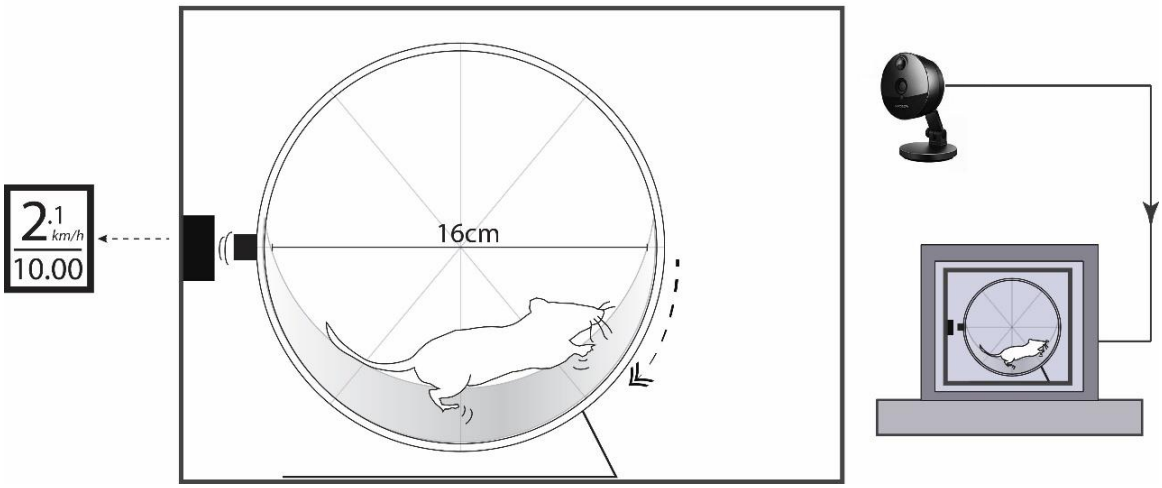

Figure 9: Overview of the setup of voluntary endurance training cages
Mice were housed individually in cages enriched with a running wheel with a sensor attached to the wheel which magnetically sent signals of each rotation to a sensor positioned on the wall of the cage. This information was digitally transmitted from the sensor to the cycle computer which displayed it as linear distance covered in km. Mice were monitored by a near infra-red camera by Foscam Client Software.

3.4 Homogenization

Tissue samples stored at -80 °C were transferred into liquid nitrogen. Tissue samples above 30 mg were pulverized in a precooled mortar and transferred into cold cell culture lysis buffer (CCLB, Promega) in a concentration of 30 mg/ml based on tissue wet weight. Samples were then homogenized with an electrical mixer (T25 basic, IKA Labortechnik) for 12- and 7-seconds with 2-minute intermission on ice to avoid excessive heating of the samples and protein degradation. Samples below 10 mg were transferred into cold lysis

buffer in a concentration of 30 mg/ml and homogenized by a 2 ml Dounce homogenizer (Kontes). All lysates were incubated on ice for 30 minutes, vortexed for 10 seconds and centrifuged at 13000 G for 1 minute at 25 °C. Supernatants were transferred into new tubes and assessed with luciferase assay and Bradford assay.

3.5 Luciferase assay

Firefly luciferase is one of the most commonly used bioluminescent reporters as it is a simple, rapid and sensitive method to study promoter activity (Williams et al., 1989). Firefly luciferase catalyzes a two-step reaction in which oxidation of D-luciferin produces a flash of light with a wavelength of approximately 550-570 nm (Figure 10). The amount of light produced is directly correlated to the quantity of luciferase given that there is an excess in substrate and ATP.

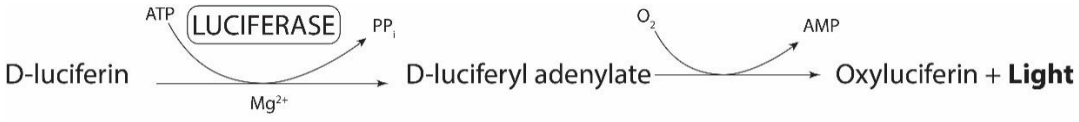

Figure 10: Production of light by luciferase
Flowchart of the reaction between luciferase and its substrate D-luciferin. First, ATP activates luciferin and gives a luciferyl-adenylate and pyrophosphate. Second, the luciferyl-adenylate reacts with oxygen and creates oxyluciferin in an electronically excited state and CO_2. When the excited-state of oxyluciferin returns to the ground state, light is released which can be detected by a luminometer. Figure adapted from Ignowski and Schaffer (2004)

Luciferase mRNA is suggested to have a short half-life of about 1.25 hours, which can be reduced to 45 minutes in presence of NO (Fan et al., 2003). A study administrating a subcutaneous injection of luciferase mRNA at the base of ear pinnae in mice showed a peak of luciferase activity at four hours followed by a gradual decay *in vivo* (Phua et al., 2013). Newly synthesized polypeptide chains of luciferase have been demonstrated *in vitro* to be catalytic competent or completely folded within a few seconds after translation is completed (Kolb et al., 1994). Further, the half-life of luciferase proteins have been reported to be three hours in cell lysates (Thompson et al., 1991), and two hours using live cells *in vitro* (Ignowski et al., 2004). Therefore, based on the mentioned reported findings on luciferase stability and activity the timepoint of muscle harvest in the present study was set to four hours.

In the present study, the luciferase reporter gene is under transcriptional regulation of NFAT with several binding sites in its promotor region. NFAT activity in NFAT-luciferase reporter mice was assessed through luciferase activity using Luciferase Assay (Promega). 30 µl of homogenate tissue samples were measured at room temperature by adding 100 µl room tempered Luciferase Assay Reagent (LAR, Promega). Samples were measured as duplicates for 10 seconds with 2-second delay at 100 % sensitivity by a luminometer (TD-20/20, Turner Designs). Readout in form of relative light units (RLU) from a standard sample consisting of lysis buffer and LAR was subtracted from all samples.

NFAT-luciferase reporter mice were initially examined for basal luciferase activity in several tissues, and muscle homogenates were further tested for enzyme kinetics under different conditions (Figure 11). Luciferase enzymes may vary in their bioluminescent output, and firefly luciferase is shown to have a flash kinetics upon addition of substrate with a rapid high signal intensity followed by fast decay of light output (Figure 11A) Luciferase stability was investigated under different storing conditions after homogenization (Figure 11B).

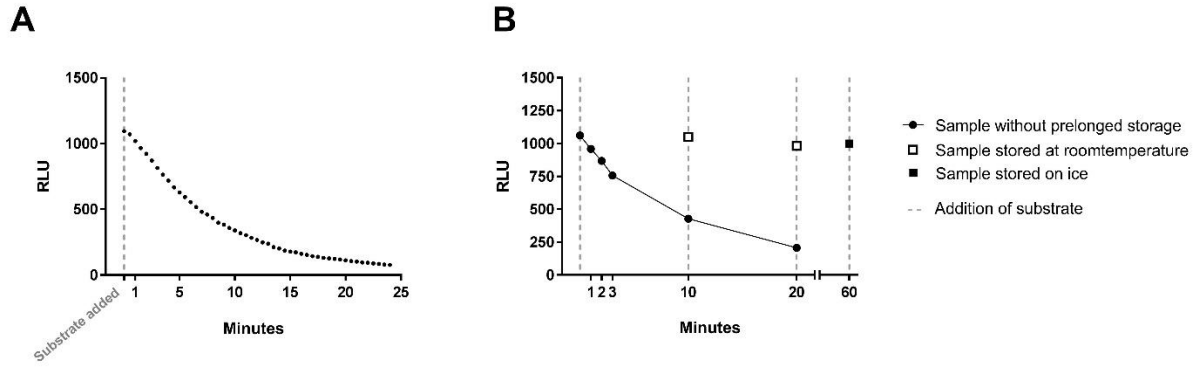

Figure 11: Enzyme kinetics in NFAT-luciferase transgenic muscle homogenates
Initial testing of luciferase kinetics from an actual muscle sample used in the experiment. (A) Substrate was added to the sample at time zero and measured every 30 seconds for 25 minutes. Light output is in concordance with flash kinetics. (B) A sample of homogenate muscle tissue was directly measured for luciferase activity by addition of substrate. This sample was then measured several times without supplement of substrate like in A (Black dots). The same sample was also checked for enzyme stability under different conditions: sample stored at room temperature at different time points (white squares), and on ice for 60 minutes (black square).

3.6 Bradford protein assay

By spectroscopic analysis, the colorimetric method of Bradford protein assay is used to measure protein concentrations in a solution (Bradford, 1976). When Bradford dye is added to the sample of unknown protein concentration, its color will change from brown/red to shades of blue depending on the concentration of the sample. As there is a linear relationship between protein concentration and the intensity of blue, a standard curve is used to calculate the protein concentration of a given sample based on the absorption value at 595 nm. Standard curves were made by measuring triplicates of a serial of dilutions of BSA in water mixed with lysis buffer (Figure 12).

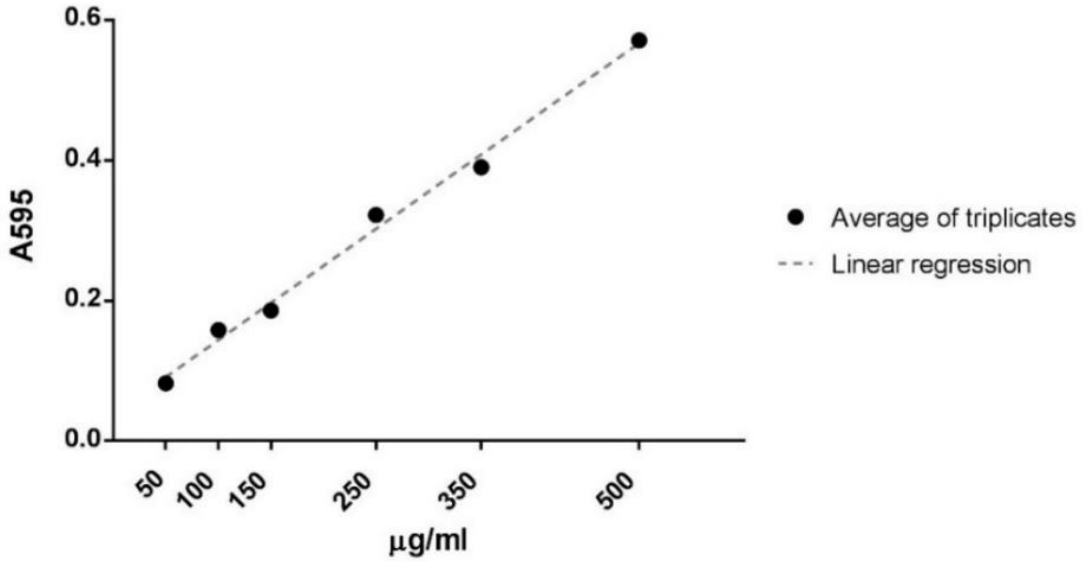

Figure 12: Standard curve used in Bradford protein assay
Standard curve of BSA with lysis buffer. Standard curve was made out of the average value of triplicates in a series of dilutions. R^2=0,993.

Bradford protein assay was used to determine protein concentration of tissue homogenates in accordance with the Bio-Rad Protein Assay Protocol (Bio-Rad) for microplates. Samples were measured as triplicates and read at 595 nm by a micro plate reader (Victor2 1420, Perkin Elmer).

3.7 Staining for β-galactosidase activity

The LacZ reporter gene in pAP-LacZ encodes the enzyme β-galactosidase which catalyzes the breakdown of X-Gal (5-bromo-4chloro-3-indolyl-ß-D-galactoside) to form indoxyl and galactose. Spontaneously dimerization of indoxyl forms an insoluble blue pigment called 5,5'-dibromo-4,4'-dichloro-indigo. LacZ-expression was used as transfection control since transfected fibers will appear blue while non-transfected fibers remain unstained (Mathiesen, 1999). Staining for β-galactosidase activity were performed by fixing whole muscles from electroporated muscles with ice-cold X-gal fixative solution (see appendix) overnight in a fume hood. After incubation, muscles were washed 3 times for 10 minutes each in PBS, followed by staining with X-Gal staining solution (see appendix) at 32°C. Lastly, muscles were washed 3 times for 5 minutes each in PBS before imaging.

3.8 Imaging

3.8.1 Fluorescence imaging of whole muscles *in vivo*

Two days after electroporation, animals were re-anesthetized with isoflurane and subsequently injected intraperitoneally with a ZRF-mixture (see appendix). The electroporated muscles, EDL and *soleus*, were surgically exposed and imaged using a camera (Canon, EOS 60D) connected to a fluorescence microscope (SZX16, Olympus). Pictures were taken in a dark room with SDFPLAPO2×PFC objective (Olympus) with XF22 filter cube to visualize EGFP transfected fibers. Afterwards, muscles were excised and slightly stretched between two pins attached to a rubber bloc followed by X-gal staining. Photo processing was conducted in Photoshop CS6.

3.8.2 Bright field imaging of muscles stained with X-gal

Bright field images of whole muscles stained for β-galactosidase activity were obtained with a camera (Canon, EOS 60D) connected to a microscope (SZX16, Olympus).

3.9 Statistical procedures

The strength training data are derived from a total of 32 animals and the contralateral leg was always used as an untrained intra-animal control. In all strength training groups n=8 with exception of three sessions of low load in *soleus* and high load in *gastrocnemius*

where n=7. The endurance training data are derived from 8 experimental animals running for 3-4 days while control data was obtained from 8 animals housed in standard cages.

For statistical comparisons of different loading regimes to contralateral untrained control leg, a two tailed Wilcoxon matched-pairs signed rank test (paired non-parametric test) was used for one- and three strength training sessions. For statistical comparisons of endurance trained mice to non-trained control mice a two tailed Mann-Whitney *U* test (unpaired non-parametric test) was used. Statistical inference for comparisons of different training forms were based on a Kruskal-Wallis H test followed by Dunn´s multiple comparisons post hoc test.

Luciferase activity in muscle tissue homogenates was measured by luciferase assay and corrected for protein concentration by Bradford assay ($RLU\mu g^{-1}$).

All statistical analysis was performed in GraphPad Prism 7 at a level of significance set to 5% ($\alpha=0.05$).

4 Results

4.1 Expression of NFAT-EGFP fusion proteins in *soleus* and EDL

After verification of *in vitro* expression of NFATc1-2-EGFP and NFATc4-EGFP fusion proteins, these expression vectors were explored *in vivo* by electroporation of *soleus* and EDL. The present study was intended to assess NFAT transcriptional activity by distinct NFAT family members in response to different strength training regimes. The hindleg muscles EDL and *soleus* in rats were chosen as a model to study fast and slow muscles, respectively.

All NFAT-EGFP fusion proteins had no/poor expression and resulted in fiber degradation. In a few observations, the electroporated muscles had some EGFP-positive fibers (Figure 13A). However, this was rarely observed and therefore the NFAT-EGFP proteins used in the present study was found unsuitable to study the nucleocytoplasmic distribution of different NFAT family members in response to strength training with different loading regimes. The backbone plasmid, pEGFP-N1 served as a positive control and had high EGFP expression and no sign of fiber degradation in all observations (Figure 13B).

As mentioned, the difference in expression levels between NFAT-EGFP fusion proteins and EGFP was very large. Therefore, the magnification needed to be customized to each muscle to enable visualization of transfected muscle fibers. Hence, the pictures are meant to illustrate the poor transfection rather than direct comparison of different protein expression levels.

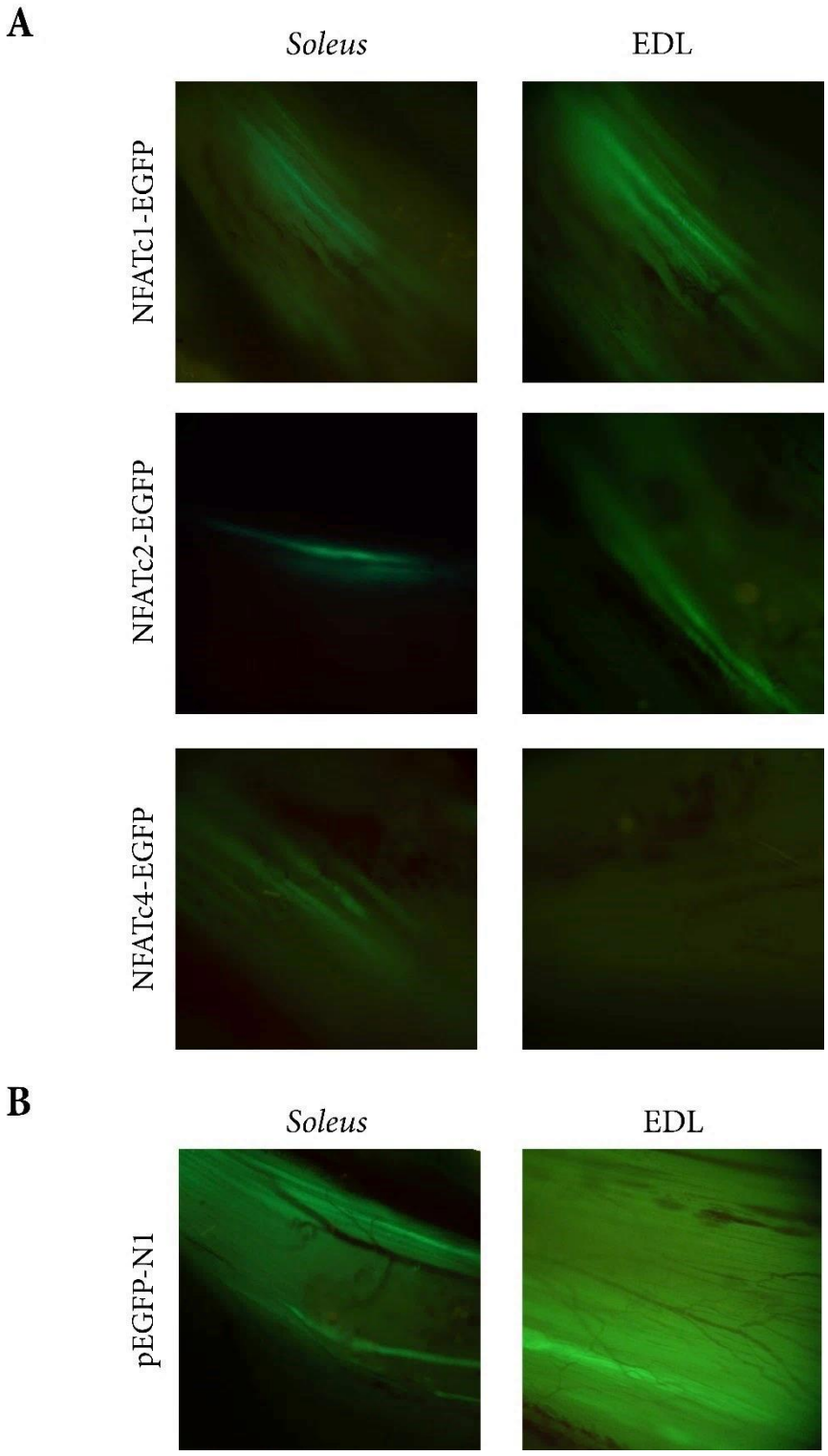

Figure 13: *In vivo* transfection of NFATc-EGFP expression vectors.

(A) The highest observed expression of the NFATc1-2-EGFP and NFATc4-EGFP fusion proteins in EDL and *soleus* examined by fluorescent microscopy at 48 hours after electroporation.
(B) The backbone plasmid pEGFP-N1 served as a positive control and had high expression levels of EGFP at all observations. Muscles electroporated with 0,9 % NaCl were used as a negative control (data not shown). Pictures are taken at different magnification in order to visualize poor expression of fusion proteins and cannot be compared directly.

4.2 Basal luciferase expression in NFAT-luciferase reporter mice

Basal NFAT activity was assessed by harvesting different tissues from control NFAT-luciferase reporter mice. The basal luciferase expression in was higher in kidney and heart compared to skeletal muscle, these results are consistent with findings reported by Wilkins et al. (2004) (Figure 14). In skeletal muscle, *soleus* was found to have higher NFAT activity compared to *gastrocnemius*. This is in agreement with studies reporting increased NFAT activity in muscles with higher proportions of slow-twitch muscle fibers (McCullagh et al., 2004; Swoap et al., 2000). Further, the transgenic region of NFAT-luciferase reporter mice was verified by sanger sequencing (performed by GATC Biotech).

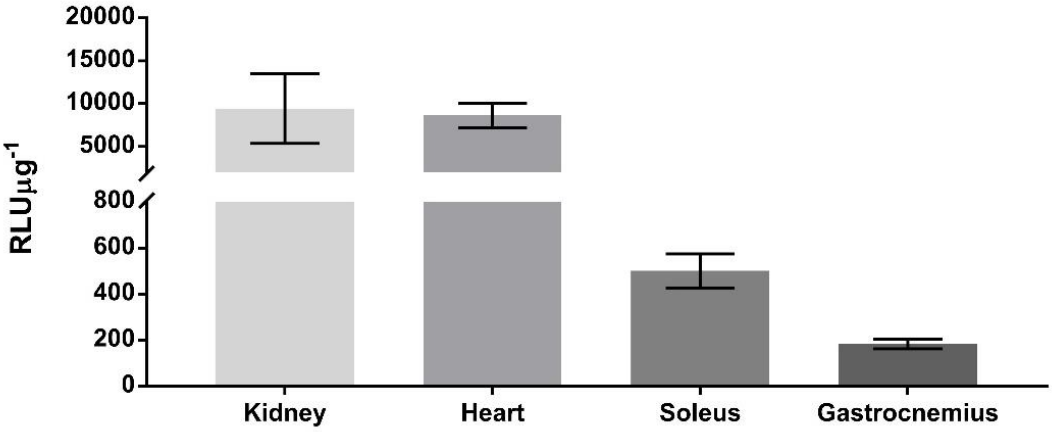

Figure 14: Verification of basal luciferase activity in NFAT-luciferase reporter mice.
Basal luciferase activity in various tissues in NFAT-luciferase reporter mice. The relative expression of different tissues is similar to previously reported findings (Wilkins et al., 2004). Error bars shown as mean±SEM; n=8.

4.3 NFAT activity in response to resistance training

In the present study, NFAT activity in response to mechanical factors was assessed by luciferase activity in NFAT-luciferase reporter mice subjected to electrically stimulated strength training. All animals performed a unilateral strength training of *gastrocnemius* and *soleus*, and the contralateral untrained leg served as an intra-animal control. Muscles of both hindlegs were harvested after four hours and analyzed with Bradford and luciferase assay.

Female transgenic NFAT-luciferase mice underwent one session of either low- or high load strength training of *soleus* and *gastrocnemius* (Figure 15). In *gastrocnemius*, luciferase activity was found non-significant different from contralateral untrained control in response to one session of strength training (Figure 15A). In *soleus*, luciferase activity in response to one session of high load was non-significant, while a significant increase was found in response to high load (Figure 15B).

Further, the effects of several strength training sessions on NFAT-activity was investigated. Mice had one day intermission between each strength training session, and muscles were harvested four hours after the last session on the fifth day. No significant increase in luciferase activity was observed in response to three strength training sessions in *gastrocnemius* and *soleus* (Figure 16).

Although resistance training only led to a significant increase in luciferase activity in *soleus*, all strength-trained groups showed a small non-significant increase relative to contralateral untrained control groups (Figure 15-16).

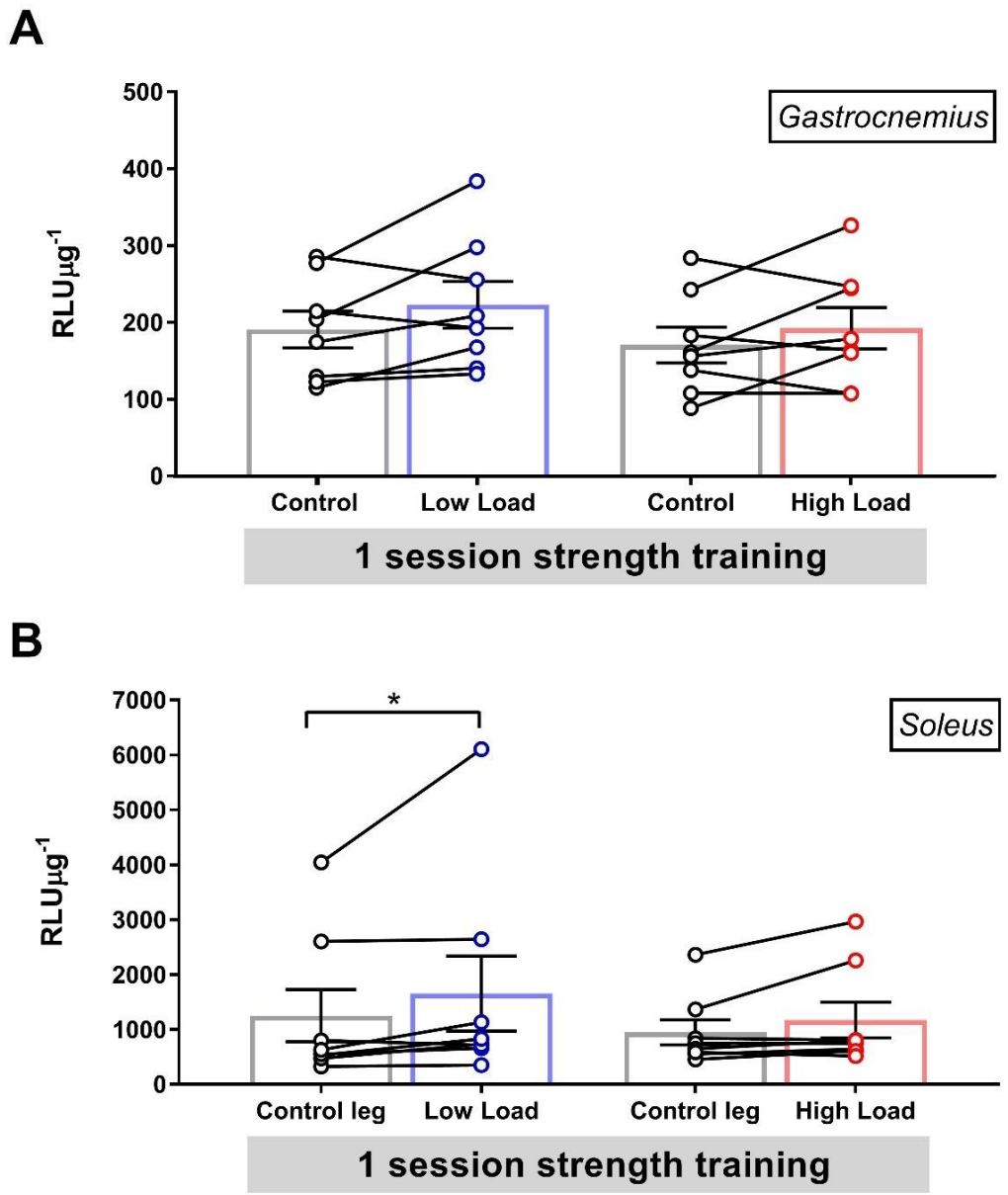

Figure 15: The effect of one strength training session in NFAT-luciferase reporter mice

Luciferase activity in *gastrocnemius* and *soleus* after one session of low and high load strength training. (A) In *gastrocnemius*, no significant difference in luciferase activity was observed after one session of high or low load strength training when compared against their respective untrained contralateral control leg. (B) In *soleus*, no significant difference in luciferase activity was observed after one session of high load when compared against untrained contralateral control leg. * denotes luciferase activity in response to low load strength training significantly different from contralateral untrained control (P=0.0391). Dots connected with a line represent muscles from the same animal. Error bars shown as mean±SEM; n=8.

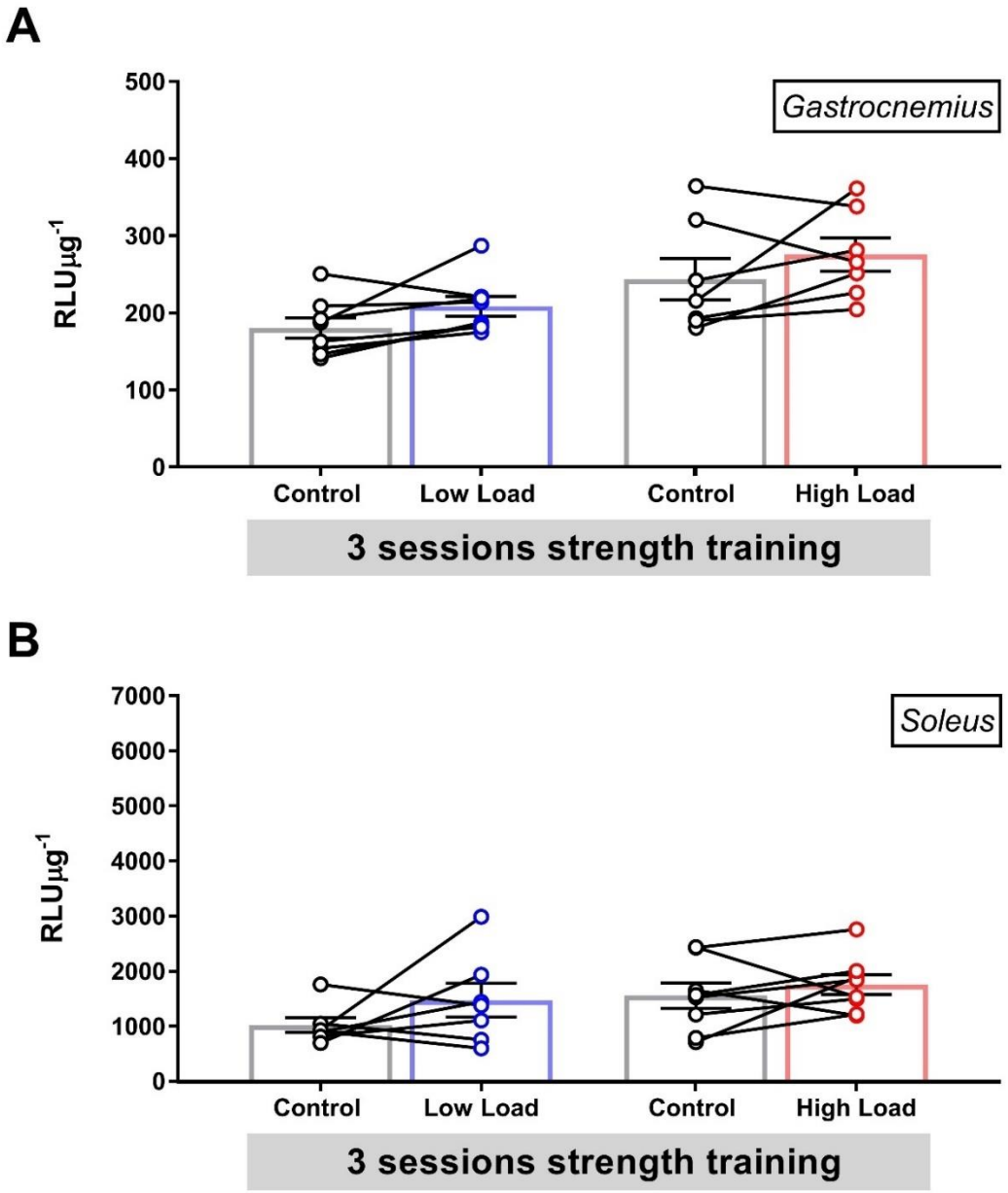

Figure 16 Non-significant increase of luciferase activity in response to three sessions of strength training in NFAT-luciferase reporter mice.

Luciferase activity in *gastrocnemius* and *soleus* four hours after the last of three sessions of high or low load strength training with one day intermission between each session. In response to three strength training sessions, no significant difference in luciferase activity was observed when comparing the different strength regimes with contralateral untrained control in either *gastrocnemius* (A) or *soleus* (B). Dots connected with a line represent muscles from the same animal. Error bars displayed as mean±SEM; n=7 for *soleus* 3 sessions low load and *gastrocnemius* 3 session high load, all other groups n=8.

4.4 Increased NFAT activity in response to endurance training

In the present study, the effect of endurance training on NFAT activity was assessed through a luciferase reporter in transgenic mice housed in cages with a running wheel connected to an ergometer. Muscles were harvested when the linear distance exceeded 10 km/night after 3-4 days and was further analyzed by Bradford and luciferase assay. Control animals were housed in cages without running wheels.

In response to endurance training, luciferase activity was found significantly different from control in both *gastrocnemius* and *soleus* (Figure 17).

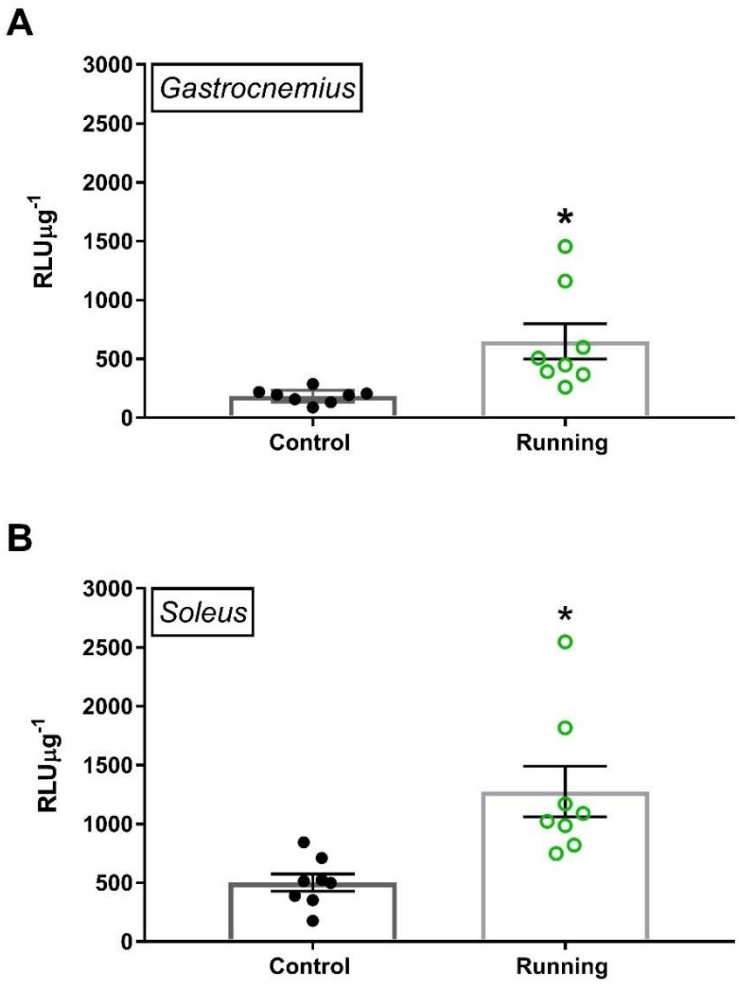

Figure 17: The effect of endurance training in NFAT-luciferase mice

Luciferase activity after exceeding a running distance of 10 km/night after 3-4 days in cages equipped with running wheel connected to an ergometer registering linear running distance. Control mice were housed in standard cages without running wheel. (A) In *gastrocnemius*, * denotes luciferase activity statistically significant different from control (P=0.0003). (B) In *soleus*, * denotes statistically significant different from control (P=0.0006). Bars show mean ±SEM; n=8.

The correlation between running distance and luciferase activity was found to be non-significant in both *gastrocnemius* and *soleus* (Figure 18). The activity pattern of a representative selection of mice (data points appointed a grey number is analyzed in Supplementary figure 1) showed large inter-animal differences which could have affected the correlation.

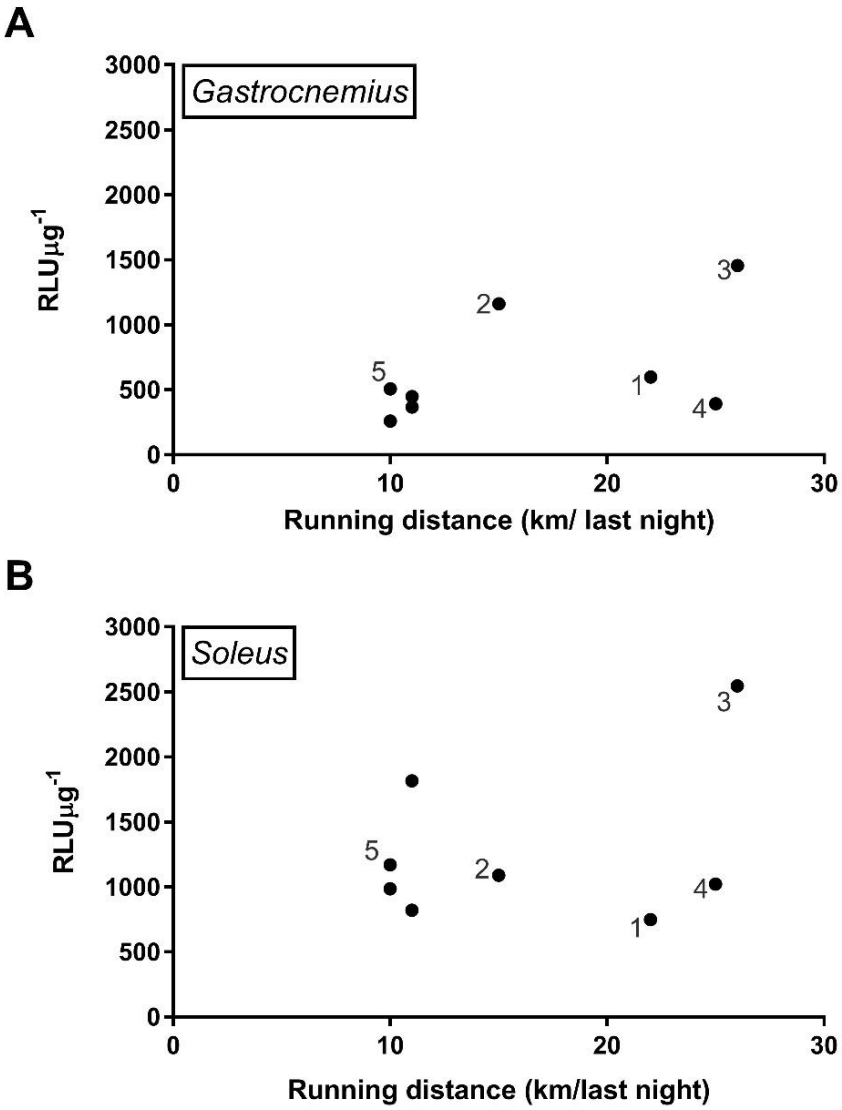

Figure 18: No correlation between running distance and luciferase activity

No significant correlation was found between running distance and luciferase activity in mice running distance of 10 km/night after 3-4 days in cages equipped with running wheel connected. The activity pattern of a representative selection of mice (data points appointed a grey number is analyzed in Supplementary figure 1) showed large inter-animal differences.

5 Discussion

One of the aims of this thesis was to investigate NFAT activity in response to different forms of exercise by elucidating the role of distinct NFAT protein family members in response to mechano-induced hypertrophy in fast and slow muscles in rats. However, since expression of the NFAT-EGFP fusion proteins led to degradation of muscle fibers *in vivo*, we were not able to conduct the intended study (section 5.1). Instead, NFAT-luciferase reporter mice were used to investigate the basal level of NFAT activity in different muscles (section 5.2), and in response to strength- (section 5.3) and endurance training (section 5.4).

NFAT activity was observed to be differently affected by strength and endurance training (Figure 19). In *gastrocnemius*, endurance training was significantly different from all strength trained groups (Figure 19A), while in *soleus*, endurance training was only significantly different from high load strength training (Figure 19B). This might be due to the difference in contraction types in the two strength training regimes. Low- and high load strength training was performed by a fast concentric- and isometric contraction, respectively. One could speculate whether fast concentric contractions is accompanied with more stretch and SACs-mediated Ca^2-influx than isometric contractions during high load. However, this proposed process remains to be confirmed.

The findings from the present study suggest that NFAT activity is mainly activated during endurance training such as running, and less during strength training. Further, increased mechanical loading during strength training seems to have no effect on NFAT activity.

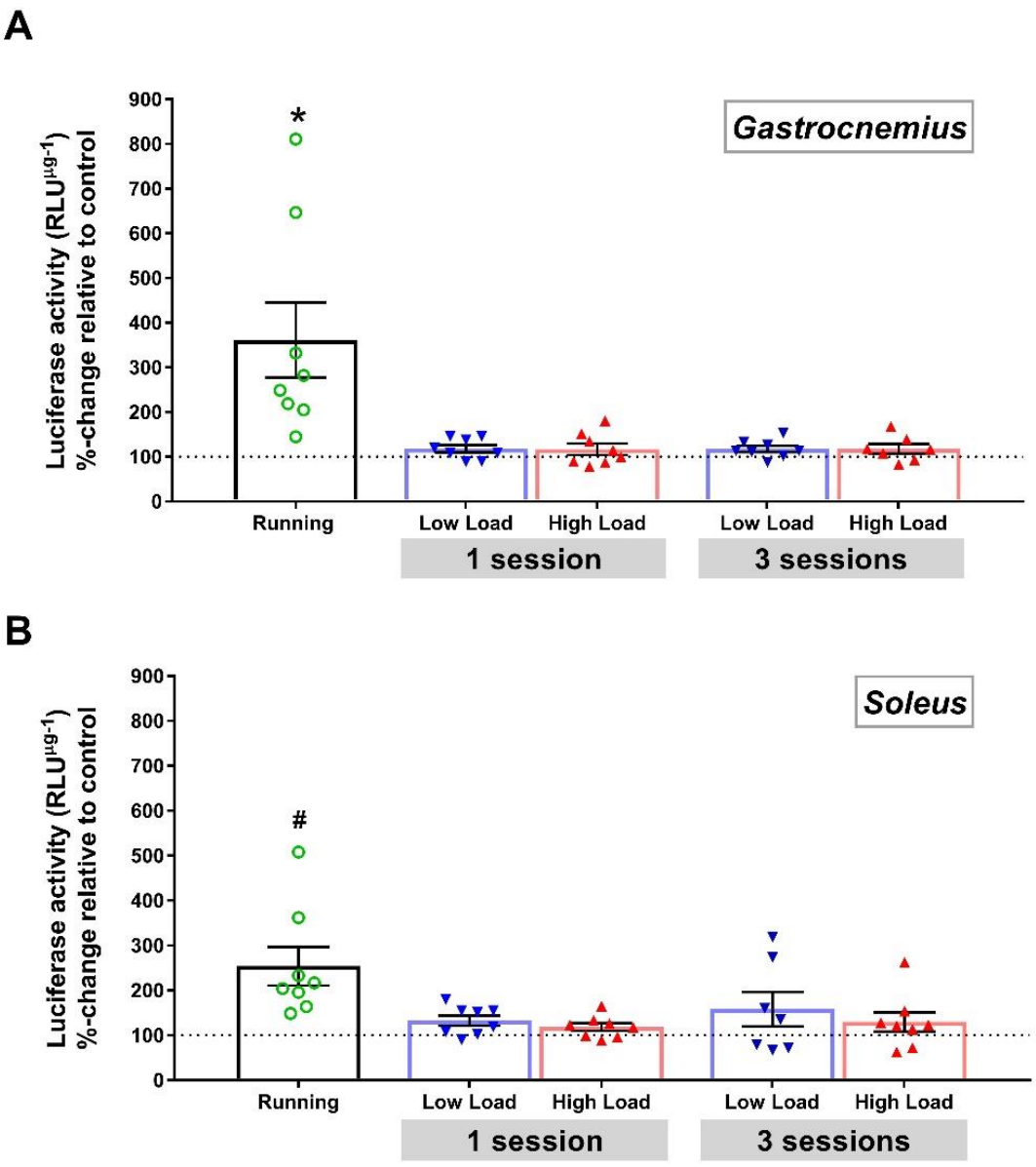

Figure 19: Comparison of luciferase activity in response to different forms of exercise

Luciferase activity (RLU$^{\mu g^{-1}}$) presented as percentage-change relative to their respective controls. For strength training experiments, RLUµg^{-1}-values of the trained leg was divided by its respective contralateral untrained control, and multiplied with 100 to get % change relative to control. For the endurance experiment, average RLUµg^{-1}-values from individual running mice were divided with the average value from sedentary mice, and then multiplied with 100 to get % change relative to control. Dotted line at 100% represent control values. No significant differences were found between different strength training regimes in either *gastrocnemius* or *soleus*. (A) In *gastrocnemius*, * denotes running group significantly different from all strength training ($P \leq 0.0185$). (B) In *soleus*, # denotes running group significantly different from high load strength training ($P \leq 0.0436$). Error bars shown as mean ± SEM; n=7 for *soleus 3 sessions low load and gastrocnemius 3 session high load, all other groups* n=8.

5.1 Degradation of muscle fibers after *in vivo* electroporation

In the present study, electroporation with verified NFAT-EGFP plasmids led to no/weak fluorescence with signs of fiber degradation in *soleus* and EDL *in vivo* (Figure 13). The NFAT-EGFP fusion proteins were intended for studying hypothesized differences in intracellular localization of distinct family members *in vivo* in response to low- and high load strength training in rats. However, the fiber degradation accompanying the expression of NFAT-EGFP fusion proteins made them unsuitable for *in vivo* studies.

Fibers expressing only EGFP did not show signs of degradation in the present study, suggesting that the expression of NFAT-EGFP fusion proteins had increased cytotoxicity. Previous unpublished findings within our research group also report degradation of transfected fibers expressing fusion proteins. Several other studies also report cytotoxicity in correlation with overexpression of GFP fusion proteins, which is suggested to be correlated with protein aggregations (H. Wang et al., 2006; H. Wang & Monteiro, 2007).

If cytotoxicity of NFAT-EGFP fusion proteins is attributed to protein aggregation, one could speculate that misfolding followed by protein aggregation could be prevented by optimization of the linker region. The fusion proteins used in the present study are cloned in frame with EGFP into the pEGFP-N1 vector from Clontech (Figure 4). The absence of a peptide linker in the fusion protein between component proteins are demonstrated to be correlated with several undesirable effects, e.g. decreased expression (Amet et al., 2009), misfolding (Arai et al., 2001), and impaired bioactivity (Bai et al., 2005; Bai & Shen, 2006). It is of great importance that NFAT proteins are in their bioactive formations as they are dependent on binding of Cn- and cooperation with transcriptional partners to translocate and gain transcriptional activity, respectively. Therefore, future localization studies should first carefully engineer a peptide linker in order to maximize expression, stability and bioactivity.

5.2 Basal NFAT activity is higher in muscles with slow phenotype

NFAT activity was confirmed to be higher in muscles with a predominance of slow-twitch fibers compared to muscles with a high proportion of fast-twitch fibers. The basal luciferase activity in *soleus* was 2-fold higher compared to *gastrocnemius* (Figure 14). This is in agreement with our hypothesis as well as other findings that reports a higher amount of NFAT proteins in *soleus* compared to EDL (McCullagh et al., 2004; Swoap et

al., 2000). Further, all NFATc1-4 family members are activated by low frequency electrical stimulation patterns that resembles the electrical activity of slow fibers (Calabria et al., 2009; Y. Liu et al., 2001). Basal luciferase activity in other tissues than muscle was in the present study also investigated (Figure 14) and were consistent with that reported by Wilkins et al. (2004), who also reported a higher activity in e.g. kidney and heart compared to skeletal muscle.

5.3 NFAT activity in response to resistance training

In the present study, one session of strength training led to a non-significant increase in NFAT activity in *gastrocnemius* (Figure 15A). Inconsistent with our hypothesis, there was no upregulation of NFAT activity after one strength training session in *gastrocnemius*. This is unexpected as other studies have indicated that NFAT has an important role in fiber type switching (Chin et al., 1998; Naya et al., 2000; S. A. Parsons et al., 2004) which is shown to occur in response to strength training regardless of load (Eftestol et al., 2016). It is therefore reasonable to assume that NFAT activity should be upregulated during strength training regardless of whether NFAT is important in load-mediated hypertrophy. Inconsistent with our hypothesis, NFAT activity is significantly upregulated after low load and not in response to high load (Figure 15B). This is in agreement with other studies that exclude the importance of NFAT activity in load mediated hypertrophy (S. A. Parsons et al., 2004). The small and mainly non-significant findings might be explained with one strength training session alone being insufficient to significantly increase NFAT activity in all trained-groups. However, NFAT activity did not increase after three strength training sessions over five days. All 8 trained-groups showed only a small non-significant increase. One could speculate whether the intermission period was too long to see an additive effect of several training sessions. To confirm this speculation, future studies should reduce the intermission time between the strength training sessions.

Non-significant results could possibly be a consequence of methodological limitations. First, conducting the present study with rats instead of mice might have produced different results. Elevated mRNA levels of RCAN1-4 which is a target gene of NFAT was found upregulated after as little as one session of high load strength training in rats receiving identical electrical stimulation (Eftestol et al, unpublished results). To exclude or confirm if there are differences in NFAT activity between rats and mice, future studies

should include both species to explore this possible difference in response to strength training. Further, it is possible that RCAN1-4 with 15 NFAT binding sites in its promotor region has a higher sensitivity towards NFAT activity compared to the luciferase reporter gene used in the present study which only has nine NFAT binding sites (Wilkins et al., 2004; J. Yang et al., 2000). Conversely, RCAN1-4 might be a poor measure of NFAT activity as expression might be affected by other transcription factors than NFAT while luciferase expression is more dependent on NFAT activity (Wilkins et al., 2004). It would be interesting to assess the mRNA levels of RCAN1-4 in the trained-groups in the present study in order to compare the present findings on NFAT activity to previous reported findings.

Lastly, muscle harvest time point might have been suboptimal in order to detect a significant change in luciferase activity. Muscles were harvested four hours after one- or three strength training session(s) and assessed for NFAT activity in muscle homogenates by luciferase assay. The time point was selected based on previous studies on luciferase stability (section 3.5). However, it is still possible that four hours was not the most optimal time point to assess luciferase activity in response to strength training. Future studies should investigate luciferase activity at several time points after strength training in order to establish the best time point for muscle harvest.

5.4 NFAT activity in response to endurance training

Endurance training led to a large increase in NFAT activity in the present study (Figure 17). This is in agreement with our hypothesis and with a previous finding that reports increased Cn activity in skeletal muscles in response to running (W. Liu et al., 2014). Endurance training is characterized by prolonged low frequency activity (Dudley et al., 1982) and all NFATc1-4 family members are shown to be activated by low frequency electrical stimulation patterns (Calabria et al., 2009; Y. Liu et al., 2001). It is therefore reasonable to assume that NFAT activity should be increased during endurance training. Further, endurance training is associated with fiber type transitions (Allen et al., 2001) and increased myoglobin levels (Hickson, 1981; Hickson & Rosenkoetter, 1981; Holloszy & Booth, 1976). These adaptations correspond with increased NFAT activity as NFAT is suggested to promote fiber type switching (Chin et al., 1998; Naya et al., 2000; S. A. Parsons et al., 2004) and myoglobin is reported to be a target gene of NFAT (Chin et al., 1998).

The strong increase observed after endurance training could be correlated to the duration of exercise. In the present study, mice ran for several hours each day, and some individuals ran as much as eight hours during the last night of the experiment. In comparison, strength trained-groups underwent one- or three 62-minute long training session(s) with a total of 540 contractions that amounted for 1.7 % of the total training time. It is possible that the difference in NFAT activity between the different training forms are due to the large difference in duration. This could be explored by having a lower limit than 10 km/night and decreasing the days' mice had access to a running wheel.

No significant correlation was found between running distance and luciferase activity (Figure 18). However, video-monitoring showed large inter-animal differences with respect to timing, speed and duration of running bouts (Supplementary figure 1), which could have affected the correlation. To overcome these proposed issues, inter-animal differences could be controlled by forced treadmill running.

The observed NFAT activity during strength- and endurance training showed that NFAT has a different activity pattern in response to different forms of exercise. In the present study, NFAT is mainly activated by endurance training and seems less affected by strength training with different loading regimes.

5.5 Conclusions

I. The NFAT-EGFP fusion proteins used in the present study were unsuitable for the intended *in vivo* localization study in response to strength training. Thus, our hypothesis regarding differential activation of NFAT between fast and slow muscles in response to varied load remains to be explored.
II. Basal activity of NFAT was confirmed higher in slow muscles compared to fast muscles.
III. NFAT activity do not increase in response to increased mechanical load, inconsistent with our hypothesis.
IV. Three strength training sessions did not increase NFAT activity compared to one session.
V. Endurance training increases NFAT activity.

6 References

Abbott, K. L., Friday, B. B., Thaloor, D., Murphy, T. J., & Pavlath, G. K. (1998). Activation and cellular localization of the cyclosporine A-sensitive transcription factor NF-AT in skeletal muscle cells. *Mol Biol Cell, 9*(10), 2905-2916.

Allen, D. L., Harrison, B. C., Maass, A., Bell, M. L., Byrnes, W. C., & Leinwand, L. A. (2001). Cardiac and skeletal muscle adaptations to voluntary wheel running in the mouse. *J Appl Physiol (1985), 90*(5), 1900-1908.

Amet, N., Lee, H. F., & Shen, W. C. (2009). Insertion of the designed helical linker led to increased expression of tf-based fusion proteins. *Pharm Res, 26*(3), 523-528. doi:10.1007/s11095-008-9767-0

Andersen, P., & Henriksson, J. (1977). Capillary supply of the quadriceps femoris muscle of man: adaptive response to exercise. *J Physiol, 270*(3), 677-690.

Arai, R., Ueda, H., Kitayama, A., Kamiya, N., & Nagamune, T. (2001). Design of the linkers which effectively separate domains of a bifunctional fusion protein. *Protein Eng, 14*(8), 529-532.

Armand, A. S., Bourajjaj, M., Martinez-Martinez, S., el Azzouzi, H., da Costa Martins, P. A., Hatzis, P., . . . De Windt, L. J. (2008). Cooperative synergy between NFAT and MyoD regulates myogenin expression and myogenesis. *J Biol Chem, 283*(43), 29004-29010. doi:10.1074/jbc.M801297200

Baar, K., & Esser, K. (1999). Phosphorylation of p70(S6k) correlates with increased skeletal muscle mass following resistance exercise. *Am J Physiol, 276*(1 Pt 1), C120-127.

Bai, Y., Ann, D. K., & Shen, W. C. (2005). Recombinant granulocyte colony-stimulating factor-transferrin fusion protein as an oral myelopoietic agent. *Proc Natl Acad Sci U S A, 102*(20), 7292-7296. doi:10.1073/pnas.0500062102

Bai, Y., & Shen, W. C. (2006). Improving the oral efficacy of recombinant granulocyte colony-stimulating factor and transferrin fusion protein by spacer optimization. *Pharm Res, 23*(9), 2116-2121. doi:10.1007/s11095-006-9059-5

Bates, D. L., Barthel, K. K., Wu, Y., Kalhor, R., Stroud, J. C., Giffin, M. J., & Chen, L. (2008). Crystal structure of NFAT bound to the HIV-1 LTR tandem kappaB enhancer element. *Structure, 16*(5), 684-694. doi:10.1016/j.str.2008.01.020

Belfield, J. L., Whittaker, C., Cader, M. Z., & Chawla, S. (2006). Differential effects of Ca2+ and cAMP on transcription mediated by MEF2D and cAMP-response element-binding protein in hippocampal neurons. *J Biol Chem, 281*(38), 27724-27732. doi:10.1074/jbc.M601485200

Benavides Damm, T., & Egli, M. (2014). Calcium's role in mechanotransduction during muscle development. *Cell Physiol Biochem, 33*(2), 249-272. doi:10.1159/000356667

Bodine, S. C., Stitt, T. N., Gonzalez, M., Kline, W. O., Stover, G. L., Bauerlein, R., . . . Yancopoulos, G. D. (2001). Akt/mTOR pathway is a crucial

regulator of skeletal muscle hypertrophy and can prevent muscle atrophy in vivo. *Nat Cell Biol, 3*(11), 1014-1019. doi:10.1038/ncb1101-1014
Bradford, M. M. (1976). A rapid and sensitive method for the quantitation of microgram quantities of protein utilizing the principle of protein-dye binding. *Anal Biochem, 72*, 248-254.
Burkholder, T. J. (2007). Mechanotransduction in skeletal muscle. *Front Biosci, 12*, 174-191.
Caiozzo, V. J., Ma, E., McCue, S. A., Smith, E., Herrick, R. E., & Baldwin, K. M. (1992). A new animal model for modulating myosin isoform expression by altered mechanical activity. *J Appl Physiol (1985), 73*(4), 1432-1440.
Calabria, E., Ciciliot, S., Moretti, I., Garcia, M., Picard, A., Dyar, K. A., . . . Murgia, M. (2009). NFAT isoforms control activity-dependent muscle fiber type specification. *Proc Natl Acad Sci U S A, 106*(32), 13335-13340. doi:10.1073/pnas.0812911106
Chin, E. R., Olson, E. N., Richardson, J. A., Yang, Q., Humphries, C., Shelton, J. M., . . . Williams, R. S. (1998). A calcineurin-dependent transcriptional pathway controls skeletal muscle fiber type. *Genes Dev, 12*(16), 2499-2509.
Clarke, M. S., Khakee, R., & McNeil, P. L. (1993). Loss of cytoplasmic basic fibroblast growth factor from physiologically wounded myofibers of normal and dystrophic muscle. *J Cell Sci, 106 (Pt 1)*, 121-133.
Coffey, V. G., & Hawley, J. A. (2007). The molecular bases of training adaptation. *Sports Med, 37*(9), 737-763.
Coleman, M. E., DeMayo, F., Yin, K. C., Lee, H. M., Geske, R., Montgomery, C., & Schwartz, R. J. (1995). Myogenic vector expression of insulin-like growth factor I stimulates muscle cell differentiation and myofiber hypertrophy in transgenic mice. *J Biol Chem, 270*(20), 12109-12116.
Conwit, R. A., Stashuk, D., Tracy, B., McHugh, M., Brown, W. F., & Metter, E. J. (1999). The relationship of motor unit size, firing rate and force. *Clin Neurophysiol, 110*(7), 1270-1275.
Crabtree, G. R., & Olson, E. N. (2002). NFAT signaling: choreographing the social lives of cells. *Cell, 109 Suppl*, S67-79.
de la Pompa, J. L., Timmerman, L. A., Takimoto, H., Yoshida, H., Elia, A. J., Samper, E., . . . Mak, T. W. (1998). Role of the NF-ATc transcription factor in morphogenesis of cardiac valves and septum. *Nature, 392*(6672), 182-186. doi:10.1038/32419
Delling, U., Tureckova, J., Lim, H. W., De Windt, L. J., Rotwein, P., & Molkentin, J. D. (2000). A calcineurin-NFATc3-dependent pathway regulates skeletal muscle differentiation and slow myosin heavy-chain expression. *Mol Cell Biol, 20*(17), 6600-6611.
Drummond, M. J., Dreyer, H. C., Fry, C. S., Glynn, E. L., & Rasmussen, B. B. (2009). Nutritional and contractile regulation of human skeletal muscle protein synthesis and mTORC1 signaling. *J Appl Physiol (1985), 106*(4), 1374-1384. doi:10.1152/japplphysiol.91397.2008
Drummond, M. J., Fry, C. S., Glynn, E. L., Dreyer, H. C., Dhanani, S., Timmerman, K. L., . . . Rasmussen, B. B. (2009). Rapamycin administration in humans blocks the contraction-induced increase in

skeletal muscle protein synthesis. *J Physiol, 587*(Pt 7), 1535-1546. doi:10.1113/jphysiol.2008.163816

Dudley, G. A., Abraham, W. M., & Terjung, R. L. (1982). Influence of exercise intensity and duration on biochemical adaptations in skeletal muscle. *J Appl Physiol Respir Environ Exerc Physiol, 53*(4), 844-850.

Dunn, S. E., Burns, J. L., & Michel, R. N. (1999). Calcineurin is required for skeletal muscle hypertrophy. *J Biol Chem, 274*(31), 21908-21912.

Eftestol, E., Egner, I. M., Lunde, I. G., Ellefsen, S., Andersen, T., Sjaland, C., . . . Bruusgaard, J. C. (2016). Increased hypertrophic response with increased mechanical load in skeletal muscles receiving identical activity patterns. *Am J Physiol Cell Physiol, 311*(4), C616-C629. doi:10.1152/ajpcell.00016.2016

Ehlers, Melissa L., Celona, B., & Black, Brian L. (2014). NFATc1 Controls Skeletal Muscle Fiber Type and Is a Negative Regulator of MyoD Activity. *Cell Reports, 8*(6), 1639-1648. doi:http://dx.doi.org/10.1016/j.celrep.2014.08.035

Faas, G. C., Raghavachari, S., Lisman, J. E., & Mody, I. (2011). Calmodulin as a direct detector of Ca2+ signals. *Nat Neurosci, 14*(3), 301-304. doi:http://www.nature.com/neuro/journal/v14/n3/abs/nn.2746.html#supplementary-information

Fan, X., Roy, E., Zhu, L., Murphy, T. C., Kozlowski, M., Nanes, M. S., & Rubin, J. (2003). Nitric oxide donors inhibit luciferase expression in a promoter-independent fashion. *J Biol Chem, 278*(12), 10232-10238. doi:10.1074/jbc.M209911200

Finsen, A. V., Lunde, I. G., Sjaastad, I., Ostli, E. K., Lyngra, M., Jarstadmarken, H. O., . . . Christensen, G. (2011). Syndecan-4 is essential for development of concentric myocardial hypertrophy via stretch-induced activation of the calcineurin-NFAT pathway. *PLoS One, 6*(12), e28302. doi:10.1371/journal.pone.0028302

Frey, N., Richardson, J. A., & Olson, E. N. (2000). Calsarcins, a novel family of sarcomeric calcineurin-binding proteins. *Proc Natl Acad Sci U S A, 97*(26), 14632-14637. doi:10.1073/pnas.260501097

Garcia-Cozar, F. J., Okamura, H., Aramburu, J. F., Shaw, K. T., Pelletier, L., Showalter, R., . . . Rao, A. (1998). Two-site interaction of nuclear factor of activated T cells with activated calcineurin. *J Biol Chem, 273*(37), 23877-23883.

Garma, T., Kobayashi, C., Haddad, F., Adams, G. R., Bodell, P. W., & Baldwin, K. M. (2007). Similar acute molecular responses to equivalent volumes of isometric, lengthening, or shortening mode resistance exercise. *J Appl Physiol (1985), 102*(1), 135-143. doi:10.1152/japplphysiol.00776.2006

Goldberg, A. L. (1968). Protein synthesis during work-induced growth of skeletal muscle. *J Cell Biol, 36*(3), 653-658.

Goldberg, A. L. (1969). Protein turnover in skeletal muscle. I. Protein catabolism during work-induced hypertrophy and growth induced with growth hormone. *J Biol Chem, 244*(12), 3217-3222.

Goldspink, D. F. (1977). The influence of immobilization and stretch on protein turnover of rat skeletal muscle. *J Physiol, 264*(1), 267-282.

Goodman, C. A., Frey, J. W., Mabrey, D. M., Jacobs, B. L., Lincoln, H. C., You, J. S., & Hornberger, T. A. (2011). The role of skeletal muscle mTOR in the regulation of mechanical load-induced growth. *J Physiol, 589*(Pt 22), 5485-5501. doi:10.1113/jphysiol.2011.218255

Graef, I. A., Chen, F., Chen, L., Kuo, A., & Crabtree, G. R. (2001). Signals transduced by Ca(2+)/calcineurin and NFATc3/c4 pattern the developing vasculature. *Cell, 105*(7), 863-875.

Graef, I. A., Gastier, J. M., Francke, U., & Crabtree, G. R. (2001). Evolutionary relationships among Rel domains indicate functional diversification by recombination. *Proc Natl Acad Sci U S A, 98*(10), 5740-5745. doi:10.1073/pnas.101602398

Graham, F. L., Smiley, J., Russell, W. C., & Nairn, R. (1977). Characteristics of a human cell line transformed by DNA from human adenovirus type 5. *J Gen Virol, 36*(1), 59-74. doi:10.1099/0022-1317-36-1-59

Gumerson, J. D., & Michele, D. E. (2011). The dystrophin-glycoprotein complex in the prevention of muscle damage. *J Biomed Biotechnol, 2011*, 210797. doi:10.1155/2011/210797

Gundersen, K. (2011). Excitation-transcription coupling in skeletal muscle: the molecular pathways of exercise. *Biol Rev Camb Philos Soc, 86*(3), 564-600. doi:10.1111/j.1469-185X.2010.00161.x

Gundersen, K., Leberer, E., Lomo, T., Pette, D., & Staron, R. S. (1988). Fibre types, calcium-sequestering proteins and metabolic enzymes in denervated and chronically stimulated muscles of the rat. *J Physiol, 398*, 177-189.

Henneman, E., Somjen, G., & Carpenter, D. O. (1965). Functional Significance of Cell Size in Spinal Motoneurons. *J Neurophysiol, 28*, 560-580.

Hennig, R., & Lomo, T. (1985). Firing patterns of motor units in normal rats. *Nature, 314*(6007), 164-166.

Hickson, R. C. (1981). Skeletal muscle cytochrome c and myoglobin, endurance, and frequency of training. *J Appl Physiol Respir Environ Exerc Physiol, 51*(3), 746-749.

Hickson, R. C., & Rosenkoetter, M. A. (1981). Separate turnover of cytochrome c and myoglobin in the red types of skeletal muscle. *Am J Physiol, 241*(3), C140-144.

Hoey, T., Sun, Y. L., Williamson, K., & Xu, X. (1995). Isolation of two new members of the NF-AT gene family and functional characterization of the NF-AT proteins. *Immunity, 2*(5), 461-472.

Hogan, P. G., Chen, L., Nardone, J., & Rao, A. (2003). Transcriptional regulation by calcium, calcineurin, and NFAT. *Genes Dev, 17*(18), 2205-2232. doi:10.1101/gad.1102703

Holloszy, J. O., & Booth, F. W. (1976). Biochemical adaptations to endurance exercise in muscle. *Annu Rev Physiol, 38*, 273-291. doi:10.1146/annurev.ph.38.030176.001421

Holz, M. K., Ballif, B. A., Gygi, S. P., & Blenis, J. (2005). mTOR and S6K1 mediate assembly of the translation preinitiation complex through dynamic protein interchange and ordered phosphorylation events. *Cell, 123*(4), 569-580. doi:10.1016/j.cell.2005.10.024

Hornberger, T. A. (2011). Mechanotransduction and the regulation of mTORC1 signaling in skeletal muscle. *Int J Biochem Cell Biol, 43*(9), 1267-1276. doi:10.1016/j.biocel.2011.05.007

Horsley, V., Friday, B. B., Matteson, S., Kegley, K. M., Gephart, J., & Pavlath, G. K. (2001). Regulation of the growth of multinucleated muscle cells by an NFATC2-dependent pathway. *J Cell Biol, 153*(2), 329-338.

Hughes, D. C., Wallace, M. A., & Baar, K. (2015). Effects of aging, exercise, and disease on force transfer in skeletal muscle. *Am J Physiol Endocrinol Metab, 309*(1), E1-E10. doi:10.1152/ajpendo.00095.2015

Huijing, P. A. (1999). Muscle as a collagen fiber reinforced composite: a review of force transmission in muscle and whole limb. *J Biomech, 32*(4), 329-345.

Huijing, P. A. (2003). Muscular Force Transmission Necessitates a Multilevel Integrative Approach to the Analysis of Function of Skeletal Muscle. *Exercise and Sport Sciences Reviews, 31*(4), 167-175.

Huxley, A. F. (1957). Muscle structure and theories of contraction. *Prog Biophys Biophys Chem, 7*, 255-318.

Ignowski, J. M., & Schaffer, D. V. (2004). Kinetic analysis and modeling of firefly luciferase as a quantitative reporter gene in live mammalian cells. *Biotechnol Bioeng, 86*(7), 827-834. doi:10.1002/bit.20059

Ingjer, F. (1979). Effects of endurance training on muscle fibre ATP-ase activity, capillary supply and mitochondrial content in man. *J Physiol, 294*, 419-432.

Jabr, R. I., Wilson, A. J., Riddervold, M. H., Jenkins, A. H., Perrino, B. A., & Clapp, L. H. (2007). Nuclear translocation of calcineurin Abeta but not calcineurin Aalpha by platelet-derived growth factor in rat aortic smooth muscle. *Am J Physiol Cell Physiol, 292*(6), C2213-2225. doi:10.1152/ajpcell.00139.2005

Janssen, I., Heymsfield, S. B., Wang, Z. M., & Ross, R. (2000). Skeletal muscle mass and distribution in 468 men and women aged 18-88 yr. *J Appl Physiol (1985), 89*(1), 81-88.

Jin, L., Sliz, P., Chen, L., Macian, F., Rao, A., Hogan, P. G., & Harrison, S. C. (2003). An asymmetric NFAT1 dimer on a pseudo-palindromic kappa B-like DNA site. *Nat Struct Biol, 10*(10), 807-811. doi:10.1038/nsb975

Kegley, K. M., Gephart, J., Warren, G. L., & Pavlath, G. K. (2001). Altered primary myogenesis in NFATC3(-/-) mice leads to decreased muscle size in the adult. *Dev Biol, 232*(1), 115-126. doi:10.1006/dbio.2001.0179

Kehlenbach, R. H., Dickmanns, A., & Gerace, L. (1998). Nucleocytoplasmic shuttling factors including Ran and CRM1 mediate nuclear export of NFAT In vitro. *J Cell Biol, 141*(4), 863-874.

Kim, E., & Guan, K. L. (2009). RAG GTPases in nutrient-mediated TOR signaling pathway. *Cell Cycle, 8*(7), 1014-1018. doi:10.4161/cc.8.7.8124

Kolb, V. A., Makeyev, E. V., & Spirin, A. S. (1994). Folding of firefly luciferase during translation in a cell-free system. *EMBO J, 13*(15), 3631-3637.

Kraemer, W. J., Patton, J. F., Gordon, S. E., Harman, E. A., Deschenes, M. R., Reynolds, K., . . . Dziados, J. E. (1995). Compatibility of high-intensity strength and endurance training on hormonal and skeletal muscle adaptations. *J Appl Physiol (1985), 78*(3), 976-989.

Linnamo, V., Moritani, T., Nicol, C., & Komi, P. V. (2003). Motor unit activation patterns during isometric, concentric and eccentric actions at different force levels. *J Electromyogr Kinesiol, 13*(1), 93-101.

Liu, W., Chen, G., Li, F., Tang, C., & Yin, D. (2014). Calcineurin-NFAT Signaling and Neurotrophins Control Transformation of Myosin Heavy Chain Isoforms in Rat Soleus Muscle in Response to Aerobic Treadmill Training. *J Sports Sci Med, 13*(4), 934-944.

Liu, Y., Cseresnyes, Z., Randall, W. R., & Schneider, M. F. (2001). Activity-dependent nuclear translocation and intranuclear distribution of NFATc in adult skeletal muscle fibers. *J Cell Biol, 155*(1), 27-39. doi:10.1083/jcb.200103020

Loewith, R., Jacinto, E., Wullschleger, S., Lorberg, A., Crespo, J. L., Bonenfant, D., . . . Hall, M. N. (2002). Two TOR complexes, only one of which is rapamycin sensitive, have distinct roles in cell growth control. *Mol Cell, 10*(3), 457-468.

Loh, C., Shaw, K. T., Carew, J., Viola, J. P., Luo, C., Perrino, B. A., & Rao, A. (1996). Calcineurin binds the transcription factor NFAT1 and reversibly regulates its activity. *J Biol Chem, 271*(18), 10884-10891.

Mathiesen, I. (1999). Electropermeabilization of skeletal muscle enhances gene transfer in vivo. *Gene Ther, 6*(4), 508-514. doi:10.1038/sj.gt.3300847

McCall, G. E., Byrnes, W. C., Dickinson, A., Pattany, P. M., & Fleck, S. J. (1996). Muscle fiber hypertrophy, hyperplasia, and capillary density in college men after resistance training. *J Appl Physiol (1985), 81*(5), 2004-2012.

McCullagh, K. J., Calabria, E., Pallafacchina, G., Ciciliot, S., Serrano, A. L., Argentini, C., . . . Schiaffino, S. (2004). NFAT is a nerve activity sensor in skeletal muscle and controls activity-dependent myosin switching. *Proc Natl Acad Sci U S A, 101*(29), 10590-10595. doi:10.1073/pnas.0308035101

Millward, D. J., Garlick, P. J., Stewart, R. J., Nnanyelugo, D. O., & Waterlow, J. C. (1975). Skeletal-muscle growth and protein turnover. *Biochem J, 150*(2), 235-243.

Miyakawa, H., Woo, S. K., Dahl, S. C., Handler, J. S., & Kwon, H. M. (1999). Tonicity-responsive enhancer binding protein, a rel-like protein that stimulates transcription in response to hypertonicity. *Proc Natl Acad Sci U S A, 96*(5), 2538-2542.

Mognol, G. P., Carneiro, F. R., Robbs, B. K., Faget, D. V., & Viola, J. P. (2016). Cell cycle and apoptosis regulation by NFAT transcription factors: new roles for an old player. *Cell Death Dis, 7*, e2199. doi:10.1038/cddis.2016.97

Moore, C. P., Rodney, G., Zhang, J. Z., Santacruz-Toloza, L., Strasburg, G., & Hamilton, S. L. (1999). Apocalmodulin and Ca2+ calmodulin bind to the same region on the skeletal muscle Ca2+ release channel. *Biochemistry, 38*(26), 8532-8537. doi:10.1021/bi9907431

Moritani, T., Muramatsu, S., & Muro, M. (1987). Activity of motor units during concentric and eccentric contractions. *Am J Phys Med, 66*(6), 338-350.

Musaro, A., McCullagh, K. J. A., Naya, F. J., Olson, E. N., & Rosenthal, N. (1999). IGF-1 induces skeletal myocyte hypertrophy through calcineurin in association with GATA-2 and NF-ATc1. *Nature, 400*(6744), 581-585.

Nader, G. A., & Esser, K. A. (2001). Intracellular signaling specificity in skeletal muscle in response to different modes of exercise. *J Appl Physiol (1985), 90*(5), 1936-1942.

Naya, F. J., Mercer, B., Shelton, J., Richardson, J. A., Williams, R. S., & Olson, E. N. (2000). Stimulation of slow skeletal muscle fiber gene expression by calcineurin in vivo. *J Biol Chem, 275*(7), 4545-4548.

Oh, M., Rybkin, II, Copeland, V., Czubryt, M. P., Shelton, J. M., van Rooij, E., . . . Rothermel, B. A. (2005). Calcineurin is necessary for the maintenance but not embryonic development of slow muscle fibers. *Mol Cell Biol, 25*(15), 6629-6638. doi:10.1128/mcb.25.15.6629-6638.2005

Okamura, H., Aramburu, J., Garcia-Rodriguez, C., Viola, J. P., Raghavan, A., Tahiliani, M., . . . Rao, A. (2000). Concerted dephosphorylation of the transcription factor NFAT1 induces a conformational switch that regulates transcriptional activity. *Mol Cell, 6*(3), 539-550.

Okamura, H., Garcia-Rodriguez, C., Martinson, H., Qin, J., Virshup, D. M., & Rao, A. (2004). A conserved docking motif for CK1 binding controls the nuclear localization of NFAT1. *Mol Cell Biol, 24*(10), 4184-4195.

Paddon-Jones, D., Sheffield-Moore, M., Cree, M. G., Hewlings, S. J., Aarsland, A., Wolfe, R. R., & Ferrando, A. A. (2006). Atrophy and impaired muscle protein synthesis during prolonged inactivity and stress. *J Clin Endocrinol Metab, 91*(12), 4836-4841. doi:10.1210/jc.2006-0651

Parsons, S. A., Millay, D. P., Wilkins, B. J., Bueno, O. F., Tsika, G. L., Neilson, J. R., . . . Molkentin, J. D. (2004). Genetic loss of calcineurin blocks mechanical overload-induced skeletal muscle fiber type switching but not hypertrophy. *J Biol Chem, 279*(25), 26192-26200. doi:10.1074/jbc.M313800200

Parsons, S. A., Wilkins, B. J., Bueno, O. F., & Molkentin, J. D. (2003). Altered Skeletal Muscle Phenotypes in Calcineurin Aα and Aβ Gene-Targeted Mice. *Mol Cell Biol, 23*(12), 4331-4343. doi:10.1128/MCB.23.12.4331-4343.2003

Pette, D., & Staron, R. S. (1990). Cellular and molecular diversities of mammalian skeletal muscle fibers. *Rev Physiol Biochem Pharmacol, 116*, 1-76.

Phua, K. K., Leong, K. W., & Nair, S. K. (2013). Transfection efficiency and transgene expression kinetics of mRNA delivered in naked and nanoparticle format. *J Control Release, 166*(3), 227-233. doi:10.1016/j.jconrel.2012.12.029

Potter, H. (1988). Electroporation in biology: methods, applications, and instrumentation. *Anal Biochem, 174*(2), 361-373.

Ramaswamy, K. S., Palmer, M. L., van der Meulen, J. H., Renoux, A., Kostrominova, T. Y., Michele, D. E., & Faulkner, J. A. (2011). Lateral transmission of force is impaired in skeletal muscles of dystrophic mice and very old rats. *J Physiol, 589*(Pt 5), 1195-1208. doi:10.1113/jphysiol.2010.201921

Rana, Z. A., Ekmark, M., & Gundersen, K. (2004). Coexpression after electroporation of plasmid mixtures into muscle in vivo. *Acta Physiol Scand, 181*(2), 233-238. doi:10.1111/j.1365-201X.2004.01282.x

Rennie, M. J., Wackerhage, H., Spangenburg, E. E., & Booth, F. W. (2004). Control of the size of the human muscle mass. *Annu Rev Physiol, 66*, 799-828. doi:10.1146/annurev.physiol.66.052102.134444

Rodney, G. G., Williams, B. Y., Strasburg, G. M., Beckingham, K., & Hamilton, S. L. (2000). Regulation of RYR1 activity by Ca(2+) and calmodulin. *Biochemistry, 39*(26), 7807-7812.

Sakuma, K., Akiho, M., Nakashima, H., Nakao, R., Hirata, M., Inashima, S., . . . Yasuhara, M. (2008). Cyclosporin A modulates cellular localization of MEF2C protein and blocks fiber hypertrophy in the overloaded soleus muscle of mice. *Acta Neuropathol, 115*(6), 663-674. doi:10.1007/s00401-008-0371-5

Schiaffino, S., & Reggiani, C. (1994). Myosin isoforms in mammalian skeletal muscle. *J Appl Physiol (1985), 77*(2), 493-501.

Schiaffino, S., & Reggiani, C. (2011). Fiber types in mammalian skeletal muscles. *Physiol Rev, 91*(4), 1447-1531. doi:10.1152/physrev.00031.2010

Semsarian, C., Wu, M. J., Ju, Y. K., Marciniec, T., Yeoh, T., Allen, D. G., . . . Graham, R. M. (1999). Skeletal muscle hypertrophy is mediated by a Ca2+-dependent calcineurin signalling pathway. *Nature, 400*(6744), 576-581. doi:10.1038/23054

Shaw, J. P., Utz, P. J., Durand, D. B., Toole, J. J., Emmel, E. A., & Crabtree, G. R. (1988). Identification of a putative regulator of early T cell activation genes. *Science, 241*(4862), 202-205.

Shen, T., Cseresnyes, Z., Liu, Y., Randall, W. R., & Schneider, M. F. (2007). Regulation of the nuclear export of the transcription factor NFATc1 by protein kinases after slow fibre type electrical stimulation of adult mouse skeletal muscle fibres. *J Physiol, 579*(Pt 2), 535-551. doi:10.1113/jphysiol.2006.120048

Shen, T., Liu, Y., Cseresnyes, Z., Hawkins, A., Randall, W. R., & Schneider, M. F. (2006). Activity- and calcineurin-independent nuclear shuttling of NFATc1, but not NFATc3, in adult skeletal muscle fibers. *Mol Biol Cell, 17*(4), 1570-1582. doi:10.1091/mbc.E05-08-0780

Silverthorn, D. U., & Johnson, B. R. (2016). *Human physiology : an integrated approach* (7th ed., global ed. ed.). Pearson: Harlow.

Spangenburg, E. E., & Booth, F. W. (2003). Molecular regulation of individual skeletal muscle fibre types. *Acta Physiol Scand, 178*(4), 413-424. doi:10.1046/j.1365-201X.2003.01158.x

Street, S. F. (1983). Lateral transmission of tension in frog myofibers: a myofibrillar network and transverse cytoskeletal connections are possible transmitters. *J Cell Physiol, 114*(3), 346-364. doi:10.1002/jcp.1041140314

Swoap, S. J., Hunter, R. B., Stevenson, E. J., Felton, H. M., Kansagra, N. V., Lang, J. M., . . . Kandarian, S. C. (2000). The calcineurin-NFAT pathway and muscle fiber-type gene expression. *Am J Physiol Cell Physiol, 279*(4), C915-924.

Talmadge, R. J., Otis, J. S., Rittler, M. R., Garcia, N. D., Spencer, S. R., Lees, S. J., & Naya, F. J. (2004). Calcineurin activation influences muscle

phenotype in a muscle-specific fashion. *BMC Cell Biol, 5*, 28. doi:10.1186/1471-2121-5-28

Terui, Y., Saad, N., Jia, S., McKeon, F., & Yuan, J. (2004). Dual role of sumoylation in the nuclear localization and transcriptional activation of NFAT1. *J Biol Chem, 279*(27), 28257-28265. doi:10.1074/jbc.M403153200

Thompson, J. F., Hayes, L. S., & Lloyd, D. B. (1991). Modulation of firefly luciferase stability and impact on studies of gene regulation. *Gene, 103*(2), 171-177.

Tidball, J. G. (2005). Mechanical signal transduction in skeletal muscle growth and adaptation. *J Appl Physiol (1985), 98*(5), 1900-1908. doi:10.1152/japplphysiol.01178.2004

Vandebrouck, A., Sabourin, J., Rivet, J., Balghi, H., Sebille, S., Kitzis, A., . . . Constantin, B. (2007). Regulation of capacitative calcium entries by alpha1-syntrophin: association of TRPC1 with dystrophin complex and the PDZ domain of alpha1-syntrophin. *FASEB J, 21*(2), 608-617. doi:10.1096/fj.06-6683com

Vega, R. B., Yang, J., Rothermel, B. A., Bassel-Duby, R., & Williams, R. S. (2002). Multiple domains of MCIP1 contribute to inhibition of calcineurin activity. *J Biol Chem, 277*(33), 30401-30407. doi:10.1074/jbc.M200123200

Vihma, H., Pruunsild, P., & Timmusk, T. (2008). Alternative splicing and expression of human and mouse NFAT genes. *Genomics, 92*(5), 279-291. doi:10.1016/j.ygeno.2008.06.011

Wang, H., Lim, P. J., Yin, C., Rieckher, M., Vogel, B. E., & Monteiro, M. J. (2006). Suppression of polyglutamine-induced toxicity in cell and animal models of Huntington's disease by ubiquilin. *Hum Mol Genet, 15*(6), 1025-1041. doi:10.1093/hmg/ddl017

Wang, H., & Monteiro, M. J. (2007). Ubiquilin overexpression reduces GFP-polyalanine-induced protein aggregates and toxicity. *Exp Cell Res, 313*(13), 2810-2820. doi:10.1016/j.yexcr.2007.04.006

Wang, N., Tytell, J. D., & Ingber, D. E. (2009). Mechanotransduction at a distance: mechanically coupling the extracellular matrix with the nucleus. *Nat Rev Mol Cell Biol, 10*(1), 75-82. doi:10.1038/nrm2594

Wang, X., Li, W., Williams, M., Terada, N., Alessi, D. R., & Proud, C. G. (2001). Regulation of elongation factor 2 kinase by p90(RSK1) and p70 S6 kinase. *EMBO J, 20*(16), 4370-4379. doi:10.1093/emboj/20.16.4370

Wilkins, B. J., Dai, Y. S., Bueno, O. F., Parsons, S. A., Xu, J., Plank, D. M., . . . Molkentin, J. D. (2004). Calcineurin/NFAT coupling participates in pathological, but not physiological, cardiac hypertrophy. *Circ Res, 94*(1), 110-118. doi:10.1161/01.RES.0000109415.17511.18

Williams, T. M., Burlein, J. E., Ogden, S., Kricka, L. J., & Kant, J. A. (1989). Advantages of firefly luciferase as a reporter gene: application to the interleukin-2 gene promoter. *Anal Biochem, 176*(1), 28-32.

Wong, T. S., & Booth, F. W. (1988). Skeletal muscle enlargement with weight-lifting exercise by rats. *J Appl Physiol (1985), 65*(2), 950-954.

Wu, H., Kanatous, S. B., Thurmond, F. A., Gallardo, T., Isotani, E., Bassel-Duby, R., & Williams, R. S. (2002). Regulation of mitochondrial biogenesis in

skeletal muscle by CaMK. *Science, 296*(5566), 349-352. doi:10.1126/science.1071163

Wu, H., Peisley, A., Graef, I. A., & Crabtree, G. R. (2007). NFAT signaling and the invention of vertebrates. *Trends Cell Biol, 17*(6), 251-260. doi:10.1016/j.tcb.2007.04.006

Wu, H., Rothermel, B., Kanatous, S., Rosenberg, P., Naya, F. J., Shelton, J. M., . . . Williams, R. (2001). Activation of MEF2 by muscle activity is mediated through a calcineurin-dependent pathway. *The EMBO Journal, 20*(22), 6414-6423. doi:10.1093/emboj/20.22.6414

Wu, Y., Collier, L., Qin, W., Creasey, G., Bauman, W. A., Jarvis, J., & Cardozo, C. (2013). Electrical stimulation modulates Wnt signaling and regulates genes for the motor endplate and calcium binding in muscle of rats with spinal cord transection. *BMC Neurosci, 14*, 81. doi:10.1186/1471-2202-14-81

Yamada, A. K., Verlengia, R., & Bueno Junior, C. R. (2012). Mechanotransduction pathways in skeletal muscle hypertrophy. *J Recept Signal Transduct Res, 32*(1), 42-44. doi:10.3109/10799893.2011.641978

Yang, J., Rothermel, B., Vega, R. B., Frey, N., McKinsey, T. A., Olson, E. N., . . . Williams, R. S. (2000). Independent signals control expression of the calcineurin inhibitory proteins MCIP1 and MCIP2 in striated muscles. *Circ Res, 87*(12), E61-68.

Yang, S. A., & Klee, C. B. (2000). Low affinity Ca2+-binding sites of calcineurin B mediate conformational changes in calcineurin A. *Biochemistry, 39*(51), 16147-16154.

Ye, Q., Feng, Y., Yin, Y., Faucher, F., Currie, M. A., Rahman, M. N., . . . Jia, Z. (2013). Structural basis of calcineurin activation by calmodulin. *Cell Signal, 25*(12), 2661-2667. doi:10.1016/j.cellsig.2013.08.033

Yeung, E. W., Whitehead, N. P., Suchyna, T. M., Gottlieb, P. A., Sachs, F., & Allen, D. G. (2005). Effects of stretch-activated channel blockers on [Ca2+]i and muscle damage in the mdx mouse. *J Physiol, 562*(Pt 2), 367-380. doi:10.1113/jphysiol.2004.075275

Zobel, C., Rana, O. R., Saygili, E., Bolck, B., Saygili, E., Diedrichs, H., . . . Schwinger, R. H. (2007). Mechanisms of Ca2+-dependent calcineurin activation in mechanical stretch-induced hypertrophy. *Cardiology, 107*(4), 281-290. doi:10.1159/000099063

7 Appendix

7.1 Appendix I: Supplementary results

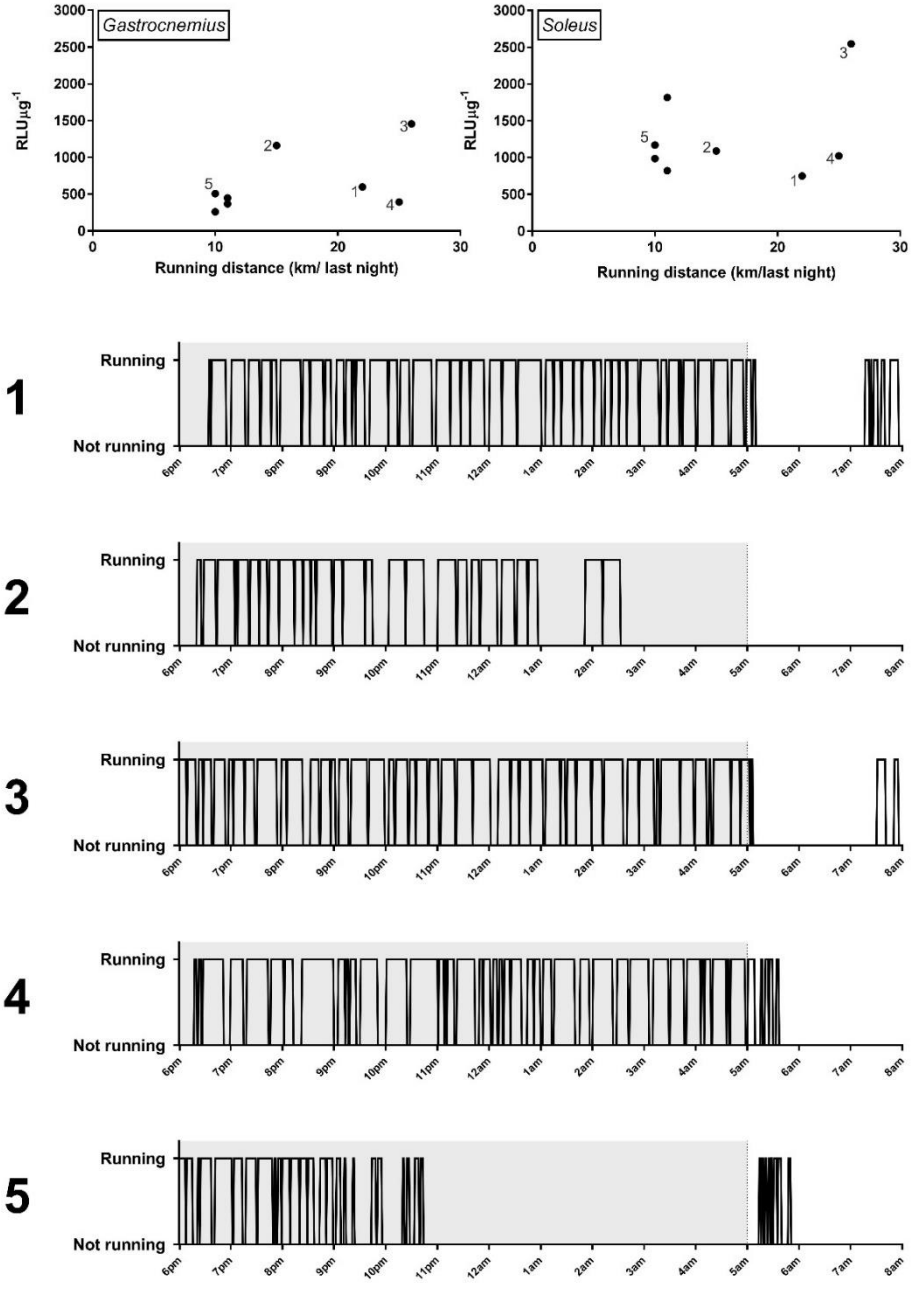

Supplementary figure 1: Activity pattern of mice during endurance training.

The activity pattern in a representative selection of mice during the last night of endurance training experiment assessed through video-monitoring. Mice displayed large inter-animal differences with respect to timing, speed and duration of running bouts. No significant correlation was observed between running distance and luciferase activity. Grey numbers correlates to black number and aligned activity pattern.

7.2 Solutions

INGREDIENTS	CONCENTRATION	VOLUME
ZRF- cocktail (Section 3.8.1)		
Zoletil Forte	250mg/ml	
Rompun	20mg/ml	3.4ml
Fentanyl	50µg/ml	8.0ml
0,9% NaCl in MQ-H_2O	0.9% NaCl	16ml
TOTAL		
Electroporation DNA solution (Section 0)		
4M NaCl	4M	4µl
dH_2O	-	46µl
Reporter DNA (lacZ)	2µg/µl	25µl
Experimental DNA (NFATc (1-4)-EGFP or pEGFP-N1	2µg/µl	25µl
TOTAL		100 µl
4 M NaCl (Section 0)		
NaCl	-	58.5 g
dH_2O	-	250 ml
TOTAL		250 ml
4 % PFA (Section 3.7, 3.2.2.1)		
PBS	1X	800 ml
Paraformaldehyde powder	-	40 g
TOTAL		800 ml
10 X PBS (Section 3.2.1, 3.7, 3.2.2.1, 3.8.2)		
NaCl	-	80.0 g
KCl	-	2.0 g
Na2HPO4 x 2 H_2O	-	14.4 g
KH4PO4	-	2.0 g
H_2O	-	1L
TOTAL		1L

INGREDIENTS	VOLUME
10 mg/ml BSA (Section 3.6)	
BSA powder	100.0 mg
dH_2O	10 ml
TOTAL	10 ml
10 X TBS (Section 3.2.2.1)	
Tris-(hydroxymetyl)aminomethane	24.25 g
NaCl	292.20 g
dH_2O	Up to 1.0 l
TOTAL	1.0 l
TBS-T (Section 3.2.2.1)	
10X TBS	100 ml
dH_2O	900 ml
Tween20	1 ml
TOTAL	1.001ml
10 % FCS in DMEM (Section 3.2.1)	
DMEM (GIBCO)	500 ml
Fetal calf serum (Bio Whittaker)	50 ml
Penicillin/Streptomycin (Bio Whittaker)	5 ml
TOTAL	555 ml
1% Agarose gel (Section 3.1)	
Agarose	1 g
1X TAE	100 ml
Ethidium bromide	2 µl
TOTAL	100ml
50X TAE (Section 3.1)	
Tris-base	242 g
Acetate (100% acetic acid):	57.1 ml
0.5M Sodium EDTA	100 ml
dH_2O	Up to 1 l
TOTAL	1.0 l

3X SDS-buffer (Section 3.2.2.1)	
0.5 M Tris HCl pH 6.8	3.75 ml
SDS	0.69 g
99.5% glycerol	3 ml
dH_2O	Up to 10 ml
Bromphenol blue	Few grains
Prior to use add 10% 1 M DTT	
X-gal fixating solution (Section 3.7)	
Formaldehyde 36% (Rectapur)	4.0ml
Glutaraldehyde 50% (EMS)	0.5ml
1X PBS, pH 7.2	196.0ml
TOTAL	200.5ml
X-gal staining solution (Section 3.7)	
0.2 M Potassium ferricyanide	30µl
0.2 M Potassium ferrocyanide	30µl
1.0 M Magnesium chloride	3µl
10X PBS (pH 6.8)	150ml
dH20	1.26ml
X-gal DMSO (50µg/µl) (Promega)	30µl
TOTAL	151.323ml

7.3 Reagents and kits

	Name	**Producer/Supplier**	**Catalog number**
Section	**Kits**		
3.1	DNA Prurification kit	Qiagen	12181
3.2.2	Lipofectamine 2000	Thermo Fisher	11668019
3.2.2	Lipofectamine 3000	Thermo Fisher	L3000001
3.5	Luciferase Assay kit	Promega	E3040
3.6	BioRad Protein Assay	BioRad	5000002
Section	**Reagents**		
3.1	Restriction enzymes (XhoI, SpeI, HindIII)	NEB	
3.1	Gel loading dye (blue 6X)	BioLabs	B7021S
3.1	1 Kb Plus DNA ladder	Thermo Fisher	10787018
3.1	Ethidium bromide	Sigma	H6501
3.2	10X DPBS	Thermo Fischer	14080055
3.2.2.1	Kaleidoscope™ Standards	Bio-Rad	1610375
3.2.2.1	Hoechst	Life tech.	H3569
3.2.2.2	Pierce™ ECL Western Blotting Substrate	Thermo Fisher	32109
3.5	QuantiLum® Recombinant Luciferase	Promega	E1701